Biomass and Bioenergy 188 (2024) 107315

Contents lists available at ScienceDirect

Biomass and Bioenergy

journal homepage: www.elsevier.com/locate/biombioe

Bio-methanol with negative CO_2 emissions from residual forestry biomass gasification: Modelling and techno-economic assessment of different process configurations

Giorgia Lombardelli [a,b,**], Roberto Scaccabarozzi [b], Antonio Conversano [a], Manuele Gatti [a,*]

[a] Politecnico di Milano, Dipartimento di Energia, Via Lambruschini 4, Milano, 20156, Italy
[b] LEAP s.c. a r.l., Via Nino Bixio 27c, Piacenza, 29121, Italy

ARTICLE INFO

Keywords:
Biomass
Gasification
Biomethanol
CCUS
Biofuels
Negative emissions

ABSTRACT

The paper presents a techno-economic comparison among five alternative process configurations for bio-methanol production from the gasification of residual forestry biomass. Process design and simulations are performed in Aspen Plus for mass and energy balance calculation, followed by preliminary sizing and economic analysis. Process schemes include a gasification island (state-of-the-art low-pressure gasification compared against a high-pressure gasifier) with syngas conditioning and compression, heat recovery, syngas composition adjustment (by CO_2 capture or addition of hydrogen produced by electrolysis), methanol synthesis and purification and a heat recovery cycle for power generation. CO_2 capture is performed with conventional chemical absorption in the benchmark cases, while low-temperature partial condensation of CO_2 is modeled in the advanced scenario. Methanol output is 14–15 kt/y in the CO_2 capture cases and 36 kt/y in the H_2 addition option.

Configurations with a pressurized gasifier and phase-change-based CO_2 separation are the most efficient ones, with a primary energy efficiency of 50 % and a Levelized Cost of Methanol (LCOM) of 700 €/t_{MeOH}. In comparison, LCOM increases to 730 €/t_{MeOH} in the case with conventional capture or between 792 €/t_{MeOH} and 831 €/t_{MeOH} (depending on the CCS technology) if the gasification pressure is conservatively reduced to 2.5 bar. In the H_2 addition scenario, LCOM increases to 821 €/t_{MeOH} due to the significant impact of the electricity consumption for H_2 production, (only partly compensated by the increased methanol production). Scenarios with CO_2 capture feature negative CO_2 emissions, in the range −1.64 to −1.84 t_{CO2eq}/t_{MeOH}, as a result of the capture and storage of biogenic CO_2 (BECCS approach).

1. Introduction

The rapid post-pandemic economic growth and the increase in global energy demand, partly satisfied by the use of fossil fuels, have caused a rise in CO_2 emissions, reaching 36.6 Gt in 2021 [1].

All relevant economic sectors should be decarbonized in a pathway towards net zero emissions by 2050 [2]. According to the Net Zero by 2050 scenario (NZE) released by the International Energy Agency (IEA), with reference to 2021 levels, global CO_2 emissions shall decrease to 21.1 Gt/y by 2030 [1]. The energy sector is expected to contribute to this reduction by more than one-third. Diffused electrification, growing efficiency, and energy-saving measures shall support decreasing the building and transport sectors energy consumption by half and one-quarter, respectively [1] while energy efficiency and fuel switching are expected to be the drivers for the reduction of the industry sector contribution.

This scenario relies on a profound transformation of the global energy mix, characterized by extensive replacement of unabated fossil fuels with low-emission sources [3]. Low-emission fuels, such as biofuels, will likely play a significant role in decarbonizing long-distance transportation and high-temperature industrial processes. The global demand for liquid biofuels forecasted by the IEA by 2030 is 5.7 Mboe/d (NZE scenario), and it is projected to remain constant until 2050 when 75 % of the produced biofuels will be consumed in aviation and shipping

* Corresponding author.
** Corresponding author. Politecnico di Milano, Dipartimento di Energia, Via Lambruschini 4, Milano, 20156, Italy.
E-mail addresses: giorgia.lombardelli@polimi.it (G. Lombardelli), manuele.gatti@polimi.it (M. Gatti).

https://doi.org/10.1016/j.biombioe.2024.107315
Received 8 July 2023; Received in revised form 18 July 2024; Accepted 20 July 2024
Available online 16 August 2024

[1].

Biofuels can be obtained with a low-carbon or CO_2-neutral pathway when their carbon is fixed from sustainable biomass or air-captured CO_2, the hydrogen they contain is obtained from renewable electricity or biomass gasification and no other major direct/indirect fossil CO_2 emissions are produced in the biofuel production process. Although their cost remains a challenge to be tackled, the interest in liquid biofuels is twofold: (i) they offer an alternative to fossil energy carriers, allowing the exploitation of the existing infrastructure and combustion equipment with limited modification requirements; (ii) they represent a strategic solution for the decarbonization of aviation and shipping, which, due to constraints on volume and weight, are dependent from liquid fuels.

Among the most attractive bio-fuels, biomethanol stands out as an interesting option due to its versatility. Indeed, methanol is currently widely employed in the chemical industry, representing one of the primary raw materials for manufacturing essential products (e.g., olefins and formaldehyde, which are at the bases of the production process of some resins and various plastics [4]). The worldwide annual methanol production has nearly doubledover the past decade, reaching about 98 Mt in 2019 [4]. Nowadays, methanol is mainly produced from fossil fuels, with the prevalent use of natural gas (about 65 % of global production) and coal (about 35 % of global production) [4]. The natural gas case requires a first step of steam reforming for syngas generation, while the coal route commonly involves a gasifier. Then, both technologies use a compression unit, a catalytic reactor, and a distillation process for methanol production and recovery. In Western European plants, the average value of direct and indirect fossil CO_2 emissions related to methanol production, in 2013, was about 0.76 t_{CO2}/t_{MeOH} [5], a figure which increases when considering a full life cycle approach.

In bio-methanol production, biomass gasification or fermentation and reforming replace fossil sources in the syngas production step [6–8]. Several bio-methanol production demonstration projects and pilot plants have received attention recently in order to test the performance and competitiveness of developing an alternative low-carbon fuel. Despite biomass gasification is a less proven technology than coal gasification, the fluidized bed technology has been demonstrated at relevant scale by collecting several thousand hours of operation in the combustion and gasification of biomass, such as bark, wood, and sludge (e.g., the large-scale plant in Guessing, Austria, and the demonstration plant in Skive, Denmark [9]). For this reason, near-atmospheric Circulating Fluidized Bed (CFB) gasification of biomass can be considered a mature technology, with open challenges related mainly to gasifier reliability (i.e., downturn time). On the other hand, even though coal-fired gasifiers are usually operated in pressurized mode (with pressures from 10 to 50 bar [10]), the pressurized operation of a biomass fluidized bed, although studied for many years [11,12], is still a topic of research at pilot and demo scale. For this reason, the scenario with a pressurized fluidized bed gasifier has been considered the most innovative, technologically challenging, and risky in the present work.

In the open literature, it is possible to find several works focused on the techno-economic evaluation of biomass to methanol plants; the most relevant studies to our research are summarized in the following. For instance, Hamelinck et al. [13] compare two gasifier technologies operating at different pressures (34.5 bar and atmospheric). In both cases, the syngas composition is corrected with the water-gas-shift reactor, and the CO_2 excess is removed with a capture system based on physical absorption (Selexol). For a plant with 400 MW_{th} of biomass thermal power input, the authors report an overall efficiency of 55%$_{HHV}$ and a price range of 8–12 $/$GJ_{HHV,\ MeOH}$ (240–360 €$_{2020}$/t_{MeOH}, escalation from 2002 costs of the original paper to 2020 costs of this study based on CEPCI). On the other hand, Galindo et al. [7] adjust the syngas composition of an atmospheric gasifier by adding hydrogen generated by water electrolysis, which is also used in an alternative biomethanol production route in combination with pure CO_2 captured from an external plant (e.g., power production); the authors report a production cost, conversion efficiency, and electric consumption in the range of 300–400 €/t_{MeOH} (382–509 €$_{2020}$/t_{MeOH}), 25–44 %, and 0.32–7 MWh/t_{MeOH}, respectively, for the biomass case, while the CO_2 route appears less attractive both form an economic and energetic point of view, with ranges of 500–600 €/t_{MeOH} (637–764 €$_{2020}$/t_{MeOH}), 17–23 %, and 9–12 MWh/t_{MeOH} for the same parameters. Clausen et al. [14] compare different process options, including biomass gasification with H_2 addition or CO_2 removal, biogas reforming, and direct CO_2 hydrogenation from captured CO_2, considering a simplified model based on chemical absorption with an amine based solvent for the CO_2 removal unit and an atmospheric gasifier. The direct hydrogenation of captured CO_2 has the worst performance, both from an efficiency and economic point of view, followed by biogas reforming. In contrast, when biomass gasification scenarios are considered, the methanol production cost and efficiency are between 11.8 and 14 €/GJ$_{HHV,\ MeOH}$ (319–378 €$_{2020}$/t_{MeOH}) and 68–72 %, respectively; furthermore, this work highlights that a significant fraction of the production cost (23–65 %) is due to the price paid for the electricity consumed. Peduzzi et al. [8] compare two different technologies of pressurized gasifiers: a fluidized bed and an entrained flow configuration, considering no hydrogen addition but CO_2 removal via chemical absorption (MEA). The two cases' overall and chemical efficiencies are similar, between 43-45 % and 45–51 %, respectively. However, the entrained flow configuration has higher equivalent efficiency derived from converting the electricity into primary energy savings using a conventional combined cycle efficiency. The sensitivity analysis on the plant size shows that increasing the biomass thermal power input from 19 MW_{th} to 200 MW_{th} reduces the methanol production cost range from 35 to 45 €/GJ$_{LHV,\ MeOH}$ (754–969 €$_{2020}$/t_{MeOH}) to 25–35 €/GJ$_{LHV,\ MeOH}$ (539–754 €$_{2020}$/t_{MeOH}). Similarly to the previous works, Hannula [15] shows that the biomass gasification route, with a gasification pressure of 4 bar and CO_2 separation via physical absorption (Rectisol), is advantageous compared to the CO_2 conversion option, with a minimum production cost of 21 €/GJ$_{LHV,\ MeOH}$ (452 €$_{2020}$/t_{MeOH}); the CO_2 conversion case is not competitive with the other options, even in case the CO_2 is available at zero cost. Hannula's work [16] considering a pressurized fluidized-bed steam/O_2-blown gasifier, compares different case studies of methanol production with CO_2 removal by Rectisol process, gasification of 5 and 22 bar and gas filtration at 550 °C and 850 °C. The case study with low-pressure gasification and high-temperature filtration has the lower cost of fuel, equal to 58.4 €/MWh$_{LHV,\ MeOH}$ (1258 €$_{2020}$/t_{MeOH}), which is 2.2 €/MWh$_{LHV,\ MeOH}$ (47 €$_{2020}$/t_{MeOH}) and 4.2 €/MWh$_{LHV,\ MeOH}$ (90 €$_{2020}$/t_{MeOH}) lower than the scenario with low-temperature filtration and high-pressure gasification. Finally, Giuliano et al. [17] optimize the CO conversion rate in the water-gas-shift reactor and the CO_2 removal rate for a system considering atmospheric gasification and physical CO_2 separation (Selexol), achieving a methanol production cost of 0.54 €/kg$_{MeOH}$ (567 €$_{2020}$/t_{MeOH}) with a CO conversion of 40 % and a CO_2 removal rate of 95 %.

Differently from the abovementioned works, in which the CO_2 capture technology is usually selected in advance, in the current paper the authors present a complete process simulation-based techno-economic assessment focused on the comparison of different methanol production schemes, considering: two gasification technologies (identified by the operative pressure); two alternative CO_2 separation systems (conventional versus innovative), comparing chemical absorption based options (respectively MEA and MDEA for the low- and high-pressure gasification cases) against a low-temperature separation system based on the partial condensation of CO_2 from syngas (hereafter also called "cryogenic" coherently with other previous studies, even though minimum temperatures are here close −50 °C, hence above the typical threshold defined by cryogenic applications), which exploits synergies with the syngas compression required for methanol synthesis; as a final case, in order to retain all the carbon content from the syngas within the methanol product, CO_2 capture is replaced by hydrogen addition from water electrolysis which is evaluated as an alternative for the syngas module

adjustment.

The present study investigates a biomass-to-methanol plant based on biomass gasification, with the aim to identify the best-performing process configuration for producing methanol among five different alternatives. A state-of-the-art low-pressure gasification design is compared with an advanced configuration featuring a high-pressure gasifier, which reduces the energy requirement for syngas compression before the subsequent methanol synthesis section. In both cases, a calibrated model, derived from the non-equilibrium one proposed by VTT for a pressurized steam/O_2-blown fluidized-bed gasifier [18], simulates syngas production by biomass gasification. Low-temperature CO_2 separation based on vapor-liquid phase-change is investigated as the innovative CO_2 removal section, given the possible synergies with the high pressure required by the downstream process and the possibility of removing only a fraction (i.e. CO_2 capture levels are not restricted to 90 %, but values close to 70 % are technically acceptable for this application) of the CO_2 in the stream sent to the MeOH synthesis reactor. Cryogenic CO_2 separation is compared to different solutions, including CO_2 absorption with benchmark MEA or MDEA solvents or the alternative route involving H_2 addition. Energy efficiency evaluation and cost analysis are then computed and discussed for the five alternative scenarios derived from different combinations of biomass gasification and syngas composition adjustment (i.e., CO_2 removal or H_2 addition) technologies.

The main original contributions from this paper are: (i) the selection of the best residual forestry biomass gasification-to-methanol option from a techno-economic standpoint after completing a detailed design, sizing, and energy and mass balance analysis; (ii) the identification of the key drivers for the plant design and performance in terms of carbon efficiency, CO_2 Capture and Storage (CCS) technology, electricity consumption, capital cost, operational cost, levelized cost of methanol, also with the support of a sensitivity analysis; (iii) the assessment of the impact of a low-temperature CO_2 separation technology compared to a conventional chemical absorption based one; (iv) the quantification of the negative CO_2 emissions potential of each CCS-based configuration analyzed.

2. Process design and plant configurations

A simplified block flow diagram of the biomass-to-methanol plant configurations is presented in Fig. 1. The dried biomass is gasified using steam and O_2 as gasification agents Oxygen is provided by an Air Separation Unit (ASU) in the CO_2 removal scenarios or by the electrolyzer when hydrogen is added to the syngas. The produced syngas is cooled down and purified from contaminants (e.g., particulate matter and sulfur compounds) before entering the composition adjustment section, featuring CO_2 removal or H_2 addition, such that the desired values of the stoichiometric module M ($(H_2–CO_2)/(CO + CO_2)$ molar ratio) is achieved at the inlet of the methanol synthesis section, which starts with syngas compression. The produced methanol is purified, generating an unconverted gas stream, recycled to the synthesis reactor, and a purged flow, burned to avoid the build-up of contaminant species (e.g., nitrogen) while recovering its thermal power content through a boiler.

Table 1 highlights the key differences between the five alternative scenarios of the investigated biomass-to-MeOH process. The distinctive features are: (i) the gasifier operative pressure, (ii) the syngas temperature at the candle filter inlet, after the gasifier, (iii) the by-pass ratio of the Water-Gas-Shift (WGS) reactor, and (iv) the syngas composition correction technology (CO_2 removal or H_2 addition).

Syngas is generated in a pressurized steam/O_2-blown fluidized-bed gasifier at 850 °C. In the low-pressure scenarios (*LOW-P(RC)* and *LOW-P*), it operates at 2.5 bar with a downstream candle filter for syngas cleaning at 550 °C, as experimentally proven and characterized by VTT [18]. On the other hand, the high-pressure scenarios (*HIGH-P(RC)* and *HIGH-P*) feature a gasification pressure of 22 bar and a downstream candle filter at 850 °C [16], representing the advanced technological options (i.e., at low Technological Readiness Level, TRL). The main benefits of these advanced technologies are: (i) the reduction of the syngas compression power requirement, and (ii) the minimization of the oxygen consumption for syngas heating after filtration (before entering

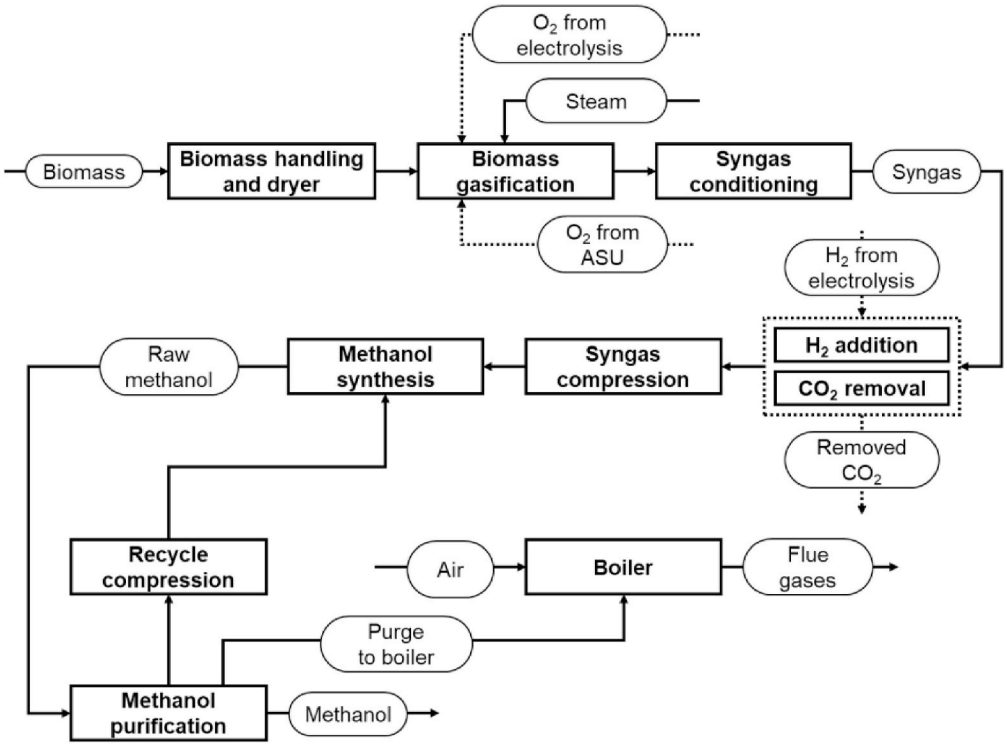

Fig. 1. Block flow diagram of the biomass to methanol plant configurations. A block flow diagram for each configuration is reported in the supplementary material with process modifications highlighted in red.

Table 1
Main features of the five investigated scenarios for the biomass-to-methanol production.

SCENARIOS	LOW-P(RC)	LOW-P	HIGH-P(RC)	HIGH-P	H_2-ADD
	"Experimentally proven" scenario -Reference case	"Experimentally proven" scenario	Advanced technological scenario - Reference case	Advanced technological scenario	Alternative scenarios with H_2 addition
Gasifier pressure	2.5 bar	2.5 bar	22 bar	22 bar	22 bar
Candle Filter	550 °C	550 °C	850 °C	850 °C	850 °C
WGS	Partial	Partial	Partial	Partial	No
CO_2 removal	MEA absorption	Low-T separation	MDEA absorption	Low-T separation	No
H_2 supply	No	No	No	No	By PEM electrolyzer

the reformer), leading to a higher LHV content in the syngas and improved energy efficiency.

The Reference Case technology for CO_2 removal (*LOW-P(RC)* and *HIGH-P(RC)*) is based on chemical absorption with solvents and compared with a new CO_2 separation unit based on partial condensation at low temperature (e.g., −50 °C) (*LOW-P* and *HIGH-P*). Monoethanolamine (MEA) is considered for *LOW-P(RC)* and methyldiethanolamine (MDEA) for *HIGH-P(RC)*, with a CO_2 removal rate of 90 % and 95 %, respectively. Since the stoichiometric module (M) at the inlet of the methanol synthesis section must be equal to 2.05 [8,19], in order to match the different capture rates of the assessed technologies (90 % or greater for solvents, while close to 70 % for cryogenic capture), a different fraction of the syngas shall be treated in the WGS reactor to increase the H_2/CO ratio before entering the CO_2 removal section. In the last scenario (*H_2-ADD*), H_2 from a grid-powered PEM electrolyzer is added to the syngas to meet to stoichiometric module constraint without using the WGS and CO_2 removal sections.

Fig. 2 shows the process flow diagram of the advanced configuration,

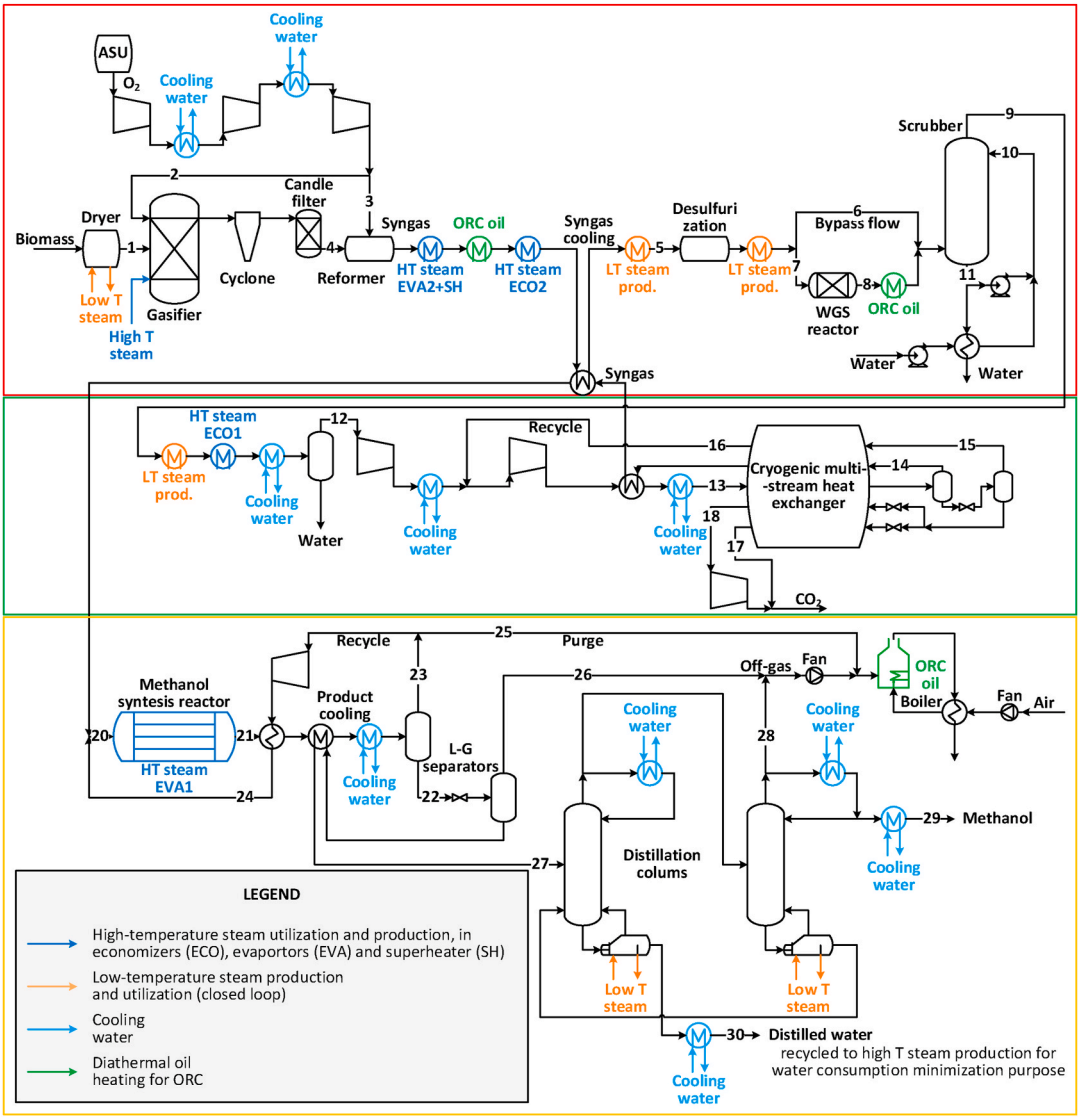

Fig. 2. Scheme of the biomass-to-methanol plant for configuration HIGH-P (red box: gasification section; green box: syngas composition correction section; yellow box: methanol synthesis section). (For interpretation of the references to colour in this figure legend, the reader is referred to the Web version of this article.)

named *HIGH-P,* involving high-pressure gasification and low-temperature CO_2 removal. The schemes of the other investigated scenarios are reported in the supplementary material. The process scheme is split into three main sections: biomass gasification (red box), syngas treatment, compression and CO_2 removal/H_2 addition (green box), and methanol synthesis (orange box).

In the first section, the wet biomass is pre-treated, dried to 13%w/w moisture content, and fed to a gasifier with oxygen from an ASU and steam produced by heat integration within the plant. The pressurized steam/O_2-blown fluidized-bed gasifier uses a cyclone and a candle filter to separate the syngas from entrained ash and unconverted char and a catalytic reformer to convert the hydrocarbons and tars. Additional oxygen is fed to the reformer to increase the syngas temperature and provide the heat required by the reforming reactions. Syngas is then cooled to 350 °C and desulphurized using a ZnO bed [20]. Subsequently, a fraction of the syngas enters the adiabatic water-gas-shift reactor at 200 °C to increase the H_2/CO molar ratio at the inlet of the subsequent methanol synthesis island. In case a different WGS configuration and catalyst would be selected, the temperature of the syngas entering the WGS reactor might be modified to meet the specifications (e.g. greater T or two stages), with limited impact on the process performance, by modulating the upstream cooling process. The WGS outlet temperature (around 367 °C) and the final CO concentration in the shifted syngas depend on the inlet syngas composition (the inlet H_2O/CO molar ratio is 1.94 for the high-pressure cases and 2.13 for the low-pressure ones) and on the chemical equilibrium conditions at the reactor exit. Even though some authors, e.g. Ref. [21], assume a temperature approach of around 10 °C with respect to the WGS equilibrium to avoid excessive catalyst amount in the bed, in this work, the CO content at the reactor outlet is between 3.1%$_{mol}$ and 3.6%$_{mol}$, depending on the scenario (see the stream tables in the supplementary material), concentration representative of a bulk conversion typically occurring in a conventional single-stage WGS [22].

Finally, the syngas enters the scrubber to remove further contaminants, such as NH_3 and HCl [21], and is sent to the syngas treatment section for compression and composition correction (i.e., capturing CO_2 to adjust the syngas module and for CCS purposes).

In the so-called "advanced" configurations, the CO_2 removal section is based on partial liquefaction of the CO_2 contained in the syngas, occurring after proper compression, refrigeration to nearly – 50 °C and separation in a flash tank. This CO_2 separation technique, described more in detail in Section 3.2 and Fig. 5, is not totally new in the field of pre-combustion CO_2 capture, where it has been proposed by Ref. [23] for coal gasification and more recently analyzed by Ref. [24] for hydrogen reforming applications, and exploits the significant volatility difference between H_2 and CO_2 in combination with a sufficiently high CO_2 partial pressure in the shifted syngas. This principle helps reaching high selectivity (CO_2 content greater than 98.5%mol in the liquid) and reasonable CO_2 removal efficiencies (ratio between the CO_2 content in the separated liquid and the total amount of CO_2 present in the syngas at the inlet of the removal unit). This CO_2 capture system is designed as follows: the saturated syngas is cooled to 40 °C and water is removed by condensation and drying before the multi-stage compression (two- and four-stage for high- and low-pressure gasification, respectively), up to 30 bar, matching the pressure of the recycled stream from the CO_2 purification flash stage (drum), and then to around 65 bar, corresponding to the inlet pressure of the downstream methanol synthesis reactor (compensating for pressure drops between the two sections). In the low-temperature multi-flow heat exchanger, the compressed syngas is cooled down to around −50 °C, using a combination of throttling and heat integration and exploiting the separated CO_2 as a refrigerant in the process (by re-evaporating and compressing it). To this purpose, part of the separated CO_2-rich liquid is throttled to 8 bar, decreasing its temperature to around −51 °C and maintaining a margin of 5 °C against CO_2 solidification and a minimum temperature approach of 3 °C in the cold-box heat exchanger, while the remaining fraction is throttled to 20 bar, export pressure selected for subsequent transport and storage. The first high-pressure flash separator aims at maximizing the CO_2 removal efficiency (i.e., higher pressure leads to higher separation). In contrast, the second low-pressure flash drum is used to increase the purity of the separated CO_2 and recover a significant fraction of the valuable fuel species, mainly H_2 and CO, dissolved in the liquid CO_2 at higher pressure (i.e., the low-pressure flash allows to further concentrate the volatile species in the vapor phase purified syngas). The vapor stream from the lower-pressure phase separator is then recycled back to the intercooled compressor. The gaseous purified syngas exiting the first separator at around 63 bar is preheated, to meet the inlet conditions of the methanol synthesis reactor, first in the multi-flow cryogenic heat exchanger, recovering cooling duty, and then collecting heat from other process streams. In the "Reference Case" scenarios (*LOW-P(RC)* and *HIGH-P (RC)*), the syngas at the exit of the gasification island is directly fed to the CO_2 removal section based on chemical absorption with solvents, and its compression is carried out downstream the CO_2 removal process before entering the methanol synthesis reactor (see supplementary material). On the other hand, in the alternative scenario with H_2 addition (*H_2-ADD*), the mixing process is performed after the intercooled compression and water condensation, taking advantage of the high operative pressure of the electrolyzer.

Methanol is produced in a water-cooled multi-tubular reactor operating at 250 °C and 60 bar, where the exothermic synthesis reactions occur [25]. The reactor product is cooled to 30 °C and fed to two flash vessels. The vent gas at the outlet of the first separator is partially recycled at the reactor inlet and partly purged to avoid the accumulation of inerts (mainly CH_4, Ar, and O_2). The second flash vessel, operating at 1 bar, separates the liquid mixture of methanol and water from the unreacted gases (mainly H_2, CO, and CO_2) [26]. Crude methanol is then purified using two distillation columns. The first separates water from methanol, and the second removes the unreacted gases [26].

The thermal demand of the process, including steam production, is satisfied by heat integration within the plant and off-gas valorization. More specifically, for the *HIGH-P* scenario (Fig. 2), syngas preheating for methanol synthesis is performed by recovering heat at the exit of the reformer and intercooled compression. Similarly, pre-heating of the recycled stream (#24) and crude methanol entering the distillation columns (#27) is carried out by cooling down the methanol reactor product. The remaining high-temperature heat, i.e., the heat generated in the methanol synthesis reactor, generates high-pressure steam for the gasifier. The available low-temperature heat produces low-pressure steam for the biomass dryer and distillation columns reboilers (ZnO bed steam consumption is considered negligible). Finally, waste heat is valorized by an Organic Rankine Cycle (ORC) used to generate electricity, recovering heat through a diathermal oil loop. The selection of an ORC over a conventional steam cycle is mainly related to the size of the heat recovery system. The electric power output generated by recovering the heat available in the plant is around 500 kW_{el}. Thus, even if the quality of the thermal power (i.e., medium/high temperature) could justify the use of steam as a working fluid, the choice of an ORC appears to be more appropriate for the selected application [27] due to the small capacity (i.e., below the MW-scale) and simpler ORC circuit, with better reliability and easier maintenance compared to the steam cycle, especially concerning the expander, which should avoid supersonic operation and bi-phase outlet conditions, also featuring a higher condensing pressure (i.e., no sub-atmospheric operation).

3. Process modelling

The investigated biomass-to-methanol plants are sized to treat about 50000 t/y (actual as received biomass input equal to 49147 t/y) of residual forestry biomass (19 MW_{LHV} plant capacity), equal to around 20 % of the availability in Parma province, estimated by ARPAE [28]. For process simulation purposes, the residual forestry biomass is defined by the biomass composition reported in Table 2, obtained from the plant

Table 2
Chemical composition and Lower Heating Value of the residual forestry biomass considered in this work.

Material	Ultimate analysis $\%_{mass,dry}$							Moisture (a.r.) %	LHV
	C	H	O	S	N	Cl	Ash		MJ/kg_{dry}
Biomass	48.84	5.94	43.79	0.04	0.24	0.03	1.12	40	18.16

species reported in the province of Parma [29] and their average chemical composition [30].

The process is simulated through Aspen Plus software [31] (version 10.1). Modelling and process design activities cover all the steps of the biomass-to-methanol plant presented in Fig. 2, including the biomass gasification section, syngas compression and CO_2 removal or H_2 addition, and the methanol synthesis and purification sections.

3.1. Gasification section

The biomass dryer operates with low-temperature steam (120 °C) and reduces the biomass moisture content from 40 % to 13 %. The electricity and thermal consumption of biomass dryer and handling system are assumed equal to 50 kJ_{el}/kg_{wet} and 150 kJ_{th}/kg_{wet} [32]. Although different solutions are possible for biomass drying, as extensively reported by Fagernäs et al. [33] (e.g., steam, hot air, and flue gases), low-temperature steam has been selected as the heat source in the present study since it can be recovered efficiently through proper heat integration with the syngas cooling line, without causing any competition with other thermal usages. Biomass is assumed to be fed to the gasifier via a lock-hopper, using a fraction of the CO_2 available from the process as the conveying medium.

The steam/O_2-blown fluidized-bed gasifier, equipped with a candle filter and reformer, is modeled with the calibrated non-equilibrium model presented in section 3.1.1, considering an operative temperature and pressure of 850 °C and 2.5 or 22 bar (depending on the scenario). Based on the pressure scenario, pressure drops in the gasifier are 0.2 or 0.4 bar, 0.2 bar in the candle filter, and 0.2 or 0.4 bar in the reformer [16]. Steam at 400 °C is produced by heat integration in the plant and fed to the gasifier to reach a steam-to-carbon molar ratio of 1 at reformer inlet [34]. In scenarios with CO_2 removal, 99 % pure oxygen is supplied by a dedicated cryogenic air separation unit (ASU), with an energy consumption of 863 kJ/kg_{O2} [35,36]. The oxygen stream is compressed to 1 bar above the gasifier pressure, maintaining its temperature below 200 °C with intercooling, and then fed to the gasifier to reach the gasification temperature, assuming $1\%_{LHV}$ thermal losses [18]. Additional O_2 is fed to the tar and hydrocarbon reformer to reach an exit temperature of 1000 °C [37]. In the *H_2-ADD* scenario, pure oxygen is provided at 26 bar and 20 °C by a PEM electrolyzed, and it is preheated in a syngas cooler to 100 °C before injection in the gasifier.

Syngas cleaning in the ZnO bed is modeled with an *RStoich* reactor block with a 3 % pressure drop. All the S/Cl/N-based compounds are converted in H_2S, HCl, and NH_3, and they are removed to trace levels by the treatments envisaged in the syngas cleaning section. The subsequential WGS section is modeled as an adiabatic reactor with an inlet temperature equal to 200 °C, reaching chemical equilibrium in the outlet stream and with a pressure drop of 0.2 or 0.4 bar (respectively, in the low- and high-pressure scenarios [16]). The WGS bypass is set to obtain a molar stoichiometric ratio M of 2.05 in the syngas entering the methanol synthesis island. In the scrubber, modeled with an Aspen *Radfrac* block, the liquid-to-gas ratio (L/G) is set to 2, the purge to 10 % of the liquid at the bottom of the column, and the pressure drop to 3 %.

3.1.1. Gasification model

The biomass gasifier has the same configuration proposed and experimentally characterized by VTT [16,18]. The gasification section is modeled in Aspen Plus with a non-equilibrium approach with the block sequence reported in Fig. 3. In the "DEC" block (*RYield*), reactor, the dry biomass is decomposed, preserving the biomass composition (ultimate analysis from Table 2), into equivalent elemental species that can be more easily managed for reaction stoichiometry calculation (hydrogen, oxygen, nitrogen, carbon, sulfur, and ash), then the moisture content is introduced ("MIX"). The "SEP" block simulates the ash and char removal, considering that a real gasifier neither reaches complete

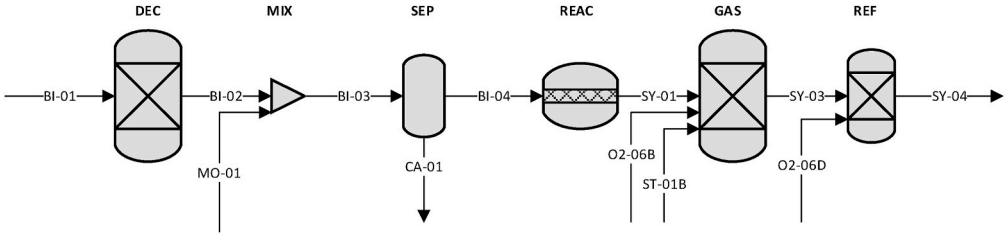

Fig. 3. Aspen-Plus simulation of the gasification section.

Table 3
Correlations applied for modelling the conversion of carbon, hydrocarbons and ammonia considering the non-equilibrium behavior of the low-pressure gasifier and reformer (T_{gas} and T_{ref} [°C]).

	Conversions related to gasification		Conversions related to reforming	
C	$+1.55E\text{-}02 \cdot T_{gas} + 8.6068E+01$	[%]		
CH_4	$-3E\text{-}03 \cdot T_{gas} + 7.074$	$[mol/kg_{bio}]$	$+2.247E\text{-}01 \cdot T_{ref} - 1.2736E+02$	[%]
C_2H_2	$-4E\text{-}05 \cdot T_{gas} + 6.454E\text{-}02$	$[mol/kg_{bio}]$	$+8.439E\text{-}01 \cdot T_{ref} - 6.3466E+02$	[%]
C_2H_4	$-2E\text{-}03 \cdot T_{gas} + 2.987$	$[mol/kg_{bio}]$	$+3.818E\text{-}01 \cdot T_{ref} - 2.3731E+02$	[%]
C_2H_6	$-1E\text{-}03 \cdot T_{gas} + 1.196$	$[mol/kg_{bio}]$	$+2.753E\text{-}01 \cdot T_{ref} - 1.4350E+02$	[%]
C_3H_8	$-1.55E\text{-}04 \cdot T_{gas} + 1.5092E\text{-}01$	$[mol/kg_{bio}]$	$+1E+02$	[%]
C_6H_6	$+2.7E\text{-}01$	$[mol/kg_{bio}]$	$+1.875E\text{-}01 \cdot T_{ref} - 7.6532E+01$	[%]
$C_{10}H_8$	$+3E\text{-}01$	$[mol/kg_{bio}]$	$+9.46E+01$	[%]
NH_3	$+4.154E\text{-}02$	$[mol/kg_{bio}]$	$+1.0679 \cdot T_{ref} - 8.9925E+02$	[%]

equilibrium nor 100 % carbon conversion. The hydrocarbon, tar, and NH_3 formation during gasification is simulated in the "REAC" block (*RStoic*), where the hydrocarbons are modeled as CH_4, C_2H_2, C_2H_4, C_2H_6, C_3H_8, and C_6H_6, the nitrogen species as NH_3 and tars as $C_{10}H_8$. As showed in Table 3, for each species, a linear function of the gasifier temperature sets the molar conversion to fit the experimental observations of syngas composition from real gasifiers. In the "GAS" block (*RGibbs*), the feed is mixed with oxygen and steam, and all the remaining compounds not specified by "REAC" are converted into equilibrium products. With this method, mass balances are automatically satisfied, while the energy balances (steady state) are computed considering the biomass LHV in input, the enthalpic contribution of each inlet/exiting stream, including the enthalpies of formation of every species. In the "REF" block (*RGibbs*), the raw syngas is partly auto-thermally reformed using additional oxygen to destroy the heavier hydrocarbons. The conversion rates of hydrocarbons, tars, and NH_3 are fixed by additional correlations based on literature experimental outcomes and functions of the outlet temperature, while the other chemical species are considered at equilibrium.

The non-equilibrium correlations (Table 3) for the low-pressure gasifier and reformer are taken from the model proposed by VTT based on experimental results of a 0.5 MW_{th} lab-scale gasifier operated with crushed wood pellets and forest residues [18] (above the temperature limits where equations would lead to conversion higher than 100 %, correlations are no longer valid and complete conversion is assumed).

For the simulation of the high-pressure gasifier, the non-equilibrium correlations expressing the conversion of carbon, hydrocarbons and ammonia are adjusted to better match the experimental observations of the CEA Grenoble Center facility on fluidized beds [38]. The experimental data reported by Valin et al. [38], reported in Table 4 in terms of Relative Yield (RY), as defined in equation (1), show the syngas composition for a gasification pressure of 2, 5, 7, and 10 bar.

$$RY_i\,[-] = \frac{Mass\ Yield\ of\ species\ i\ at\ High\ P}{Mass\ Yield\ f\ species\ i\ at\ 2\ bar} \tag{1}$$

The RY is a function of the pressure and can be expressed through equation (2), where the parameters a and b, reported in Table 5, are calibrated to fit the experimental data by Valin et al. [38]. Fig. 4 shows the good agreement between the experimental value of RY (dots) and the output of equation (2) (lines).

$$RY\,[-] = a \cdot P^b \tag{2}$$

The non-equilibrium correlations for the gasifier and reformer at high pressure, are reported in Table 6. Carbon conversion in the gasifier is set to the value suggested by VTT at 22 bar (i.e., 96 %) [16], while, for the other species, conversion is calculated by multiplying the low-pressure conversion (Table 3) and the Relative Yield (equation (2)). The species not included in the experimental data of the high-pressure gasification model (C_3H_8, $C_{10}H_8$, and NH_3) are assumed at equilibrium. On the other hand, the reformer conversions at high pressure are estimated assuming the same distance from the equilibrium of the low-pressure case.

Table 4
Relative Yield (RY) of hydrocarbons at high-pressure gasification (5, 7 and 10 bar) compared to 2 bar.

P [bar]	2	5	7	10
RY_{CH4}	1.00	1.25	1.31	1.38
RY_{C2H2}	1.00	0.09	0.09	0.09
RY_{C2H4}	1.00	0.50	0.45	0.40
RY_{C2H6}	1.00	1.50	2.00	2.25
RY_{C6H6}	1.00	1.21	1.25	1.29

Table 5
Calibrated coefficients for the equation of the Relative Yield function of gasifier pressure.

Coefficient	a	b
CH_4	0.8889	0.1964
C_2H_2	4.269	−2.097
C_2H_4	1.532	−0.6332
C_2H_6	0.6843	0.5233
C_6H_6	0.9045	0.1696

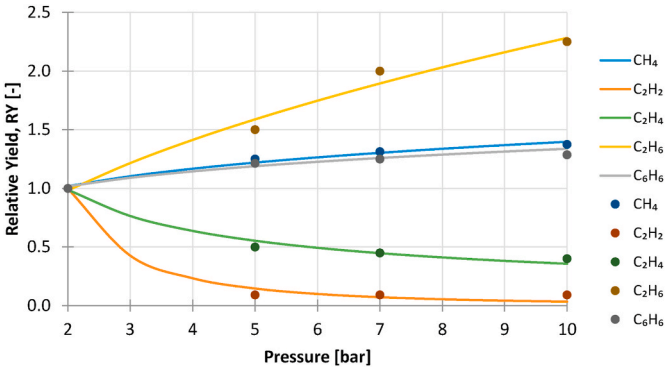

Fig. 4. Comparison of the RY from the calibrated model (lines) and the RY experimental results (dots).

3.2. Syngas compression and CO_2 capture or H_2 addition

Referring to Figs. 1 and 2, the conditioned and shifted syngas (#9) after scrubbing and heat recovery enters the CO_2 capture or H_2 addition section. The condensed water is removed in an adiabatic and isobaric flash at 40 °C. Then, syngas compression is modeled using compressors with isentropic and mechanical efficiencies equal to 0.78 and 0.95, respectively, with intercooling at 40 °C. The minimum temperature difference in the coolers is 10 °C, and the pressure drop is 3 % of the inlet pressure. A cooling tower supplies cooling water to the plant with an electrical consumption equal to 1.5 % of the thermal power transferred to the environment and a makeup of 5 % of the total cooling water flow rate.

The low-temperature phase-change CO_2 separation is performed in the cryogenic (i.e., operating at a low temperature but always greater than the triple point of CO_2) multi-streams heat exchanger equipped with a double-flash system. The scheme of the CO_2 separation system is reported in Fig. 5. The capture system works through sequential compression and cooling before the cryogenic heat exchanger, where the CO_2-rich syngas enters at 40 °C and 65 bar and is cooled down to −48 °C. Then, the double flash system separates the syngas (mainly H_2 and CO) from the liquefied CO_2 exploiting the volatility difference between CO_2 and other mixture components. The first flash works at −48 °C and around 64 bar and separates the lean-CO_2 syngas (vapor phase) from the CO_2-rich liquid stream, which is depressurized to 30 bar and sent to the second flash. The scheme is auto-refrigerated, since the cooling duty required is provided via throttling the CO_2 liquid streams, which are then heated while cooling down the feed stream: the liquid stream of CO_2 (around 98.5%$_{mol}$ CO_2 including slightly less than 1%$_{mol}$ CO and H_2) leaving the second flash is split and furtherly depressurized to 20 bar and 8 bar, and re-introduced in the cryogenic heat exchanger. The temperature difference in the heat exchanger is set to 2 °C slightly varying the fraction of the CO_2 stream depressurized to around 8 bar and then repressurized to 20 bar (pressure of CO_2 storage). The lean-CO_2 syngas separated from the first flash is re-introduced in the cryogenic heat exchanger and heated up to 25 °C. The vapor stream from the second flash is recycled back in the system after heat integration in the cryogenic heat exchanger. The CO_2 separation system achieves CO_2

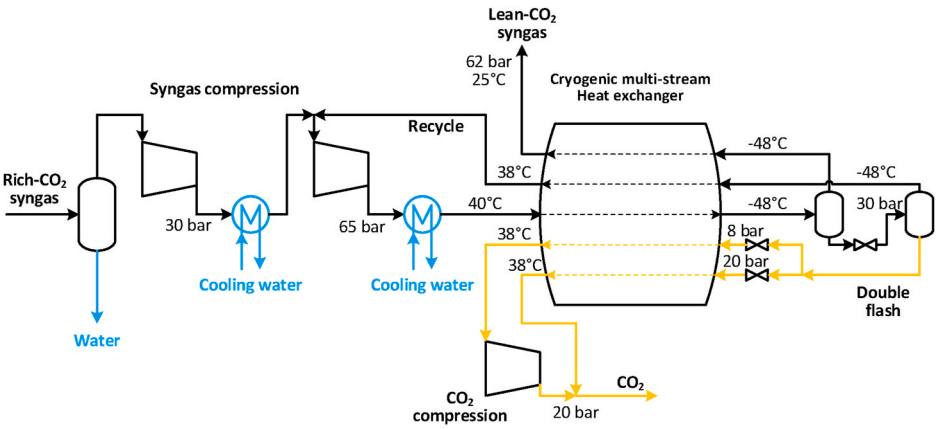

Fig. 5. Scheme of the CO_2 separation system based on low-temperature vapor-liquid phase-change including compressors, a cryogenic multi-stream heat exchanger, throttling valves for auto-refrigeration and phase separators.

Table 6
Correlations applied for modelling the conversion of carbon, hydrocarbons and ammonia considering the non-equilibrium behavior of the high-pressure gasifier and reformer.

	Conversions related to gasification		Conversions related to reforming	
C	96	[%]		
Species i	$Conv_{i,\ LowP} \cdot RY_i$	[mol/kg_{bio}]	$Conv_{i,\ LowP} \cdot Conv_{i,\ HighP,Equil}/Conv_{i,\ LowP,Equil}$	[%]

capture rates (expressed as the ratio of moles of CO_2 captured by the process to the total mole of CO_2 in the feed stream) in the range 67–70 % in the investigated scenarios, depending on the CO_2 concentration in the shifted syngas stream, with a thermal duty of the cryogenic multi-stream heat exchanger close to 150 kWh/t_{CO2}, assuming a highly compact plate-type configuration (e.g., plate and fin or printed circuit).

The first version of a phase-change-based CO_2 separation technology for pressurized syngas streams was initially proposed in Ref. [23]. The current scheme has been modified by eliminating the expanders of the lean-CO_2 syngas, since the stream is needed at 60 bar for the downstream process, and producing the CO_2 stream at 20 bar. The equation of state used for the simulation of this unit is the Peng-Robinson equation as calibrated by Fandino et al. [39].

In conventional absorption with MEA, the syngas is treated in an absorber where aqueous monoethanolamine enters at the top and selectively absorbs CO_2 via slightly exothermic reaction. The CO_2-loaded solvent is then preheated (lean/rich heat exchanger) and enters the stripper, where the captured CO_2 is desorbed by supplying thermal energy to the solution, and the regenerated CO_2-lean solvent is finally cooled via heat recovery in a lean/rich heat exchanger and recycled back to the absorber. The MEA technology (adopted for the base case low pressure gasifier) operates at nearly ambient pressure (i.e., 1.4 bar), and the reboiler works at 110–125 °C [40]. Given the high technological maturity of CO_2 capture based on MEA, this section is simulated as a black box where 90 % of CO_2 is removed from the syngas stream, and the electrical consumption and thermal duty of the process are respectively 0.075 MJ_{el}/kg_{CO2} and 3.3 MJ_{th}/kg_{CO2}, provided by steam at 130–140 °C [40].

In the absorption with MDEA, CO_2 is removed through chemical absorption by amine scrubbing with an aqueous solution of methyldiethanolamine operating at 17.6 bar. The stripper for solvent regeneration operates at 1.2 bar, with a reboiler working at 109 °C. For the MDEA-based CO_2 removal section the CO_2 capture rate is set to 95 %, the electric consumption to 0.048 MJ_{el}/kg_{CO2}, and the thermal duty of the reboiler to 1.50 MJ_{th}/kg_{CO2}, provided by steam at 120 °C (in accordance with the literature [41,42]).

The reported electrical consumptions of both chemical absorption cases do not include the compression power for the captured CO_2, which is added separately.

In the scenarios with H_2 addition (*H_2-ADD*), H_2 is produced by a grid-powered PEM electrolyzer with a specific consumption of 4.9 kWh/Nm^3_{H2}, operating at 26 bar and 20 °C. Hydrogen is compressed to match the methanol synthesis pressure and added to the syngas to reach M = 2.05.

3.3. Methanol synthesis

The compressed syngas at the outlet of the syngas treatment section is heated to 210 °C [43] at the methanol reactor inlet. Methanol synthesis occurs in a multi-tubular reactor with a conventional Cu/Zn/Al_2O_3 catalyst in the tubes cooled by boiling water at 250 °C. The supplementary material details the Graaf et al. [44,45] modeling approach followed for evaluating the performance of the conventional methanol reactor.

The separation of the products leaving the methanol reactor is simulated in two adiabatic flash in series, the first operating at the same pressure of the reactor and the second one operating at 1 bar. The separated liquid stream is mainly comprised of methanol and water, which are then separated in two distillation units modeled (using the *RadFrac* operation block) in Aspen Plus. The distillation columns are designed as reported in Nyari et al. [26], with the reflux ratio and boilup ratio adjusted in each of the five scenarios to obtain high-purity methanol (>99.85%$_{mass}$) [46] at the top of the second column and pure water at the bottom of the first column. Crude methanol at 87 °C and atmospheric pressure enters the first distillation column, operating with a reboiler at around 100 °C and generating pre-purified methanol at the top and water at the bottom. The pre-purified methanol enters the second distillation column, where the top condenser removes the residual nonreacted gases from the methanol, while the water-rich bottom, leaving the reboiler at around 70 °C, is recycled to the first column.

In the methanol synthesis section, the thermodynamic model selected is Peng-Robinson with calibrated binary interaction parameters to appropriately simulate the solubility of the unreacted gases (CO, H_2 and CO_2) in the condensed liquid phase (water and methanol) at the

outlet of the methanol synthesis reactor (more details on the selected equation of state are reported in Ref. [47]).

4. Economic analysis

The economic analysis aims to evaluate the Levelized Cost of Methanol (*LCOM*) for the five different scenarios, i.e., the breakeven selling price that, at the end of the plant lifetime, repays the CAPEX and OPEX costs, while generating financial interests and by producing a certain amount of methanol [34]. *LCOM* is computed according to equation (3) where *CAPEX* is the total capital plant expenditure, *OPEX* is the operational expenditure, *CCF* is the Capital Charge Factor (assumed equal to 0.094, i.e., corresponding to a discount rate equal to 8 % and a life of the plant set at 25 years), m_{MeOH} is the hourly production rate of methanol and h are the plant equivalent hours (assumed equal to 7884 operating hours per year, i.e., corresponding to a capacity factor of 0.90).

$$LCOM = \frac{CAPEX \cdot CCF + OPEX}{m_{MeOH} \cdot h} \tag{3}$$

The total capital expenditure (*CAPEX*) is evaluated as the sum of the capital cost associated to the equipment design, engineering, procurement and construction (EPC), including contingencies and owners costs (overnight cost expressed in base-year €). For the main plant components (listed in Table 7) the associated equipment cost $C_{i,eq}$, including also the direct and indirect labor costs for construction and installation and the supporting facilities costs (bare erected cost), is evaluated in accordance with equation (4). The cost is estimated on the base of reference cost C_i^0 applied to the equipment with size S_i^0 reported in reference sources/previous studies, and the actual size of the equipment S_i; the bare erected cost C_i^0, and reference size S_i^0 of the equipment and the scale parameter n are reported in Table 7.

$$C_{i,eq} = C_i^0 \cdot \left(\frac{S_i}{S_i^0} \right)^n \tag{4}$$

The evaluation of the capital cost related to each piece of equipment, $C_{i,tot}$, is carried out as from equation (5) requiring factors such as EPC_i and OC_i other than the equipment cost $C_{i,eq}$. *EPC* accounts for the costs of services provided by the engineering, procurement and construction contractor and project and process contingencies; *OC* includes the owner's cost such as pre-production, financial costs and inventory capital. The *EPC* and *OC* factors are applied to each equipment as a percentage of the bare erected equipment cost $C_{i,eq}$, taking references from the literature as reported in Table 7 (for some equipment the *EPC* and *OC* are not reported since they are already included in C_i^0).

$$C_i = C_{i,eq} \cdot \left(1 + \frac{EPC_i}{100}\right) \cdot \left(1 + \frac{OC_i}{100}\right) \tag{5}$$

Finally, costs are escalated to the selected base year (2020). The escalation is conducted on the basis of the *CEPCI* (Chemical Engineering Plant Cost Index) values, to account for the effect of inflation, as reported in equation (6), where $C_{i,2020}$ is the actual cost, $CEPCI_{ref}$ is the index in reference year, $C_{ref,i}$ the cost in reference year, $CEPCI_{2020}$ the current index referred to year 2020 ($CEPCI_{2020}$ = 596.2 [56]).

$$C_{i,2020} = C_i \cdot \left(\frac{CEPCI_{2020}}{CEPCI_{ref}} \right) \tag{6}$$

The cost of the equipment not reported in Table 7 is evaluated, after sizing with the cost functions reported by Turton et al. [57]. According to Turton methodology, the purchase cost of each equipment (at ambient operating pressure and with carbon steel material) is evaluated on the basis of the size parameter and then converted into the bare module cost (to account for direct and indirect costs, specific materials of construction and operating pressure) and the grass root cost (accounting for installation costs and contingencies); this procedure is used for the methanol synthesis section including the reactor, the distillation columns,the heat exchanger, as well as for the fan, pump and flash separator. The cost of the methanol synthesis reactor is estimated assuming a heat exchanger with fixed tubes in stainless steel (shell and tube) operating at high pressure.

The operational expenditure (*OPEX*) is the sum of the cost of biomass, consumables and utilities, the operating labor cost and other fixed operational cost related to maintenance, insurance and administrative and support labor. OPEX includes.

- cost of biomass equal to 68 €/$t_{bio\ dry}$, i.e., around 3.74 €/GJ (Italian average price for logging residues from thinning from conifer trees from Ref. [58]),
- cost of electricity with a price of 0.083 €/kWh [59], representative of the average industrial price for electricity,
- cost for transport and storage of the captured CO_2 equal to 10 €/t_{CO2} [60],
- process water, with a price of 1.4 €/m^3 [57],

Table 7
Reference cost items, i.e., purchase cost C^0, EPC and owner's cost factors for the main equipment units.

Equipment	S^0 (Reference capacity)		C^0 (Reference bare erected cost)		n (scale factor)	EPC	OC	Ref.
ASU	76.6	t_{O2}/h	47.8	M€	0.5	52 %	20 %	[16]
O_2 compressor	10	MW_{el}	5.7	M€	0.67	52 %	20 %	[16]
Biomass handling	157	$MW_{LHV\ bio}$	5.3	M€	0.31	52 %	20 %	[16]
Biomass dryer	0.427	$kg_{wat.rem}$/s	1.7	M€	0.5	52 %	20 %	[16]
Low-P gasifier	11.6	$kg_{bio\ dry}$/s	23.8	M€	0.75	52 %	30 %	[16]
Low-P filter	1.466	$kmol_{syn}$/s	5.9	M€	0.67	52 %	30 %	[16]
Low-P reformer	1.32	$kmol_{syn}$/s	14.1	M€	0.67	52 %	20 %	[16]
High-P gasifier, filter and reformer	815	$MW_{LHV\ bio}$	198.8	M$	0.67	15.5 %	0 %	[21]
Desulfurization	413.82	$MW_{LHV\ in}$	0.66	M€	0.67	14 %	15 %	[48]
WGS	815	$MW_{LHV\ in}$	3.36	M$	0.67	15.5 %	0 %	[21]
Scrubber	1.47	$kmol_{syn}$/s	5	M€	0.67	52 %	30 %	[16]
Syngas compressor	10	MW_{el}	6.34	M$	0.67	0 %	32 %	[21]
Cryogenic multi-streams heat exchanger	106.364	kW/K	0.165	M€	0.9	100 %	32 %	[49]
MEA section	833.33	Nm^3_{in}/h	2.583	M€	0.6	-[b]	-[b]	[50]
MDEA section	204803	Nm^3_{in}/h	40.5	M€	0.6	40 %	-[b]	[51]
Electrolyzer	10	MW_{el}[a]	10	M€	0.73	-[b]	-[b]	[52,53]
Boiler	355	MW_{th}	52	M$	1	46.72 %	27 %	[21]
ORC	375	kW_{el}	1.575	M€	0.66	-[b]	-[b]	[54]
Cooling system	4000	kW_{th}	0.157	M$	0.67	14 %	14 %	[55],[c]

[a] The electrolyzer cost is increased by 15 % [43,53] to account one reconditioning of stack during the plant life time.
[b] *EPC* and *OC* are not reported because already included in C_i^0.
[c] Estimation carried out using Thermoflex by Thermoflow.

Table 8
Main results of the simulations for the five alternative biomass-to-methanol scenarios. BECCS stands for BioEnergy with CCS (meaning that the CO_2 captured and sent to storage is of biogenic origin). When net fossil CO_2 emissions are negative it means that CO_2 is indirectly removed from the atmosphere according to a Carbon Dioxide Removal (CDR) approach.

SCENARIOS		LOW-P (RC)	LOW-P	HIGH-P (RC)	HIGH-P	H_2-ADD
Biomass	t/y	49147	49147	49147	49147	49147
MeOH produced	t/y	14481	14449	15435	15337	36083
CGE	%	69.3	67.2	74.7	72.1	75.9
$\eta_{primary,en}$	%	42.9	43.8	50.1	50.3	33.3
Electricity consumption	kW	+2255	+2542	+1586	+1585	+28353
Electricity production (ORC)	kW	0	−540	−351	−439	−442
Net electric import from the grid	kW	+2255	+2002	+1235	+1146	+27911
WGS bypass	%	58	17	69	16	100
Syngas at MeOH synthesis loop inlet	kmol/h	206	222	203	237	509
CO_2 in the syngas at MeOH synthesis loop inlet	$\%_{mol}$	5	17	2	17	13
CO_2 capture rate	%	90	71	95	67	–
Biogenic CO_2 captured (BECCS)	t/y	30954	30850	27913	27829	–
Net fossil CO_2 emissions	t_{CO2}/t_{MeOH}	−1.81	−1.84	−1.64	−1.66	+1.64
H_2 added	t/y	–	–	–	–	3907
Carbon efficiency[a]	%	37.6 %	37.6 %	40.1 %	39.9 %	93.8 %

[a] Ratio between the amount of carbon in the produced methanol divided by the carbon in the biomass feedstock.

- catalyst for methanol synthesis with a price of 15 €/kg [61] and replaced after 2 years of operation [62].

The labor cost is estimated assuming 12 operators in the plant and an average wage equal to 45000 €/y/operator. The fixed *OPEX* and the O&M costs (e.g., additional consumables, component replacement) not previously specified have been estimated as a lump sum 4 % of the total *CAPEX* ([21,63]).

5. Results and discussion

5.1. Process simulation results

The main results of the process simulation are reported in Table 8 for the five alternative scenarios. The Cold Gas Efficiency (*CGE*) is evaluated as reported in equation (7), where the syngas mass flow rate, m_{syngas}, and Lower Heating Value, LHV_{syngas}, refer to the syngas at the inlet of the methanol synthesis loop (before H_2 addition in the *H_2-ADD* scenario). Therefore, the reported value of *CGE* includes the contribution of gasification, reforming, syngas cleaning, Water Gas Shift and CO_2 removal. The primary energy efficiency, $\eta_{primary,en}$, is defined as the ratio between the energy content of the produced methanol and the total plant energy input, which is the sum of the primary energy content of biomass and the plant electricity consumption, as reported in equation (8), where the electricity is divided by the average efficiency of the Italian thermoelectric sector (0.495 [64]) for adequate conversion into primary energy

$$CGE = \frac{m_{syngas} \cdot LHV_{syngas}}{m_{biomass} \cdot LHV_{biomass}} \tag{7}$$

$$\eta_{primary,en} = \frac{m_{MeOH} \cdot LHV_{MeOH}}{m_{biomass} \cdot LHV_{biomass} + \left(\frac{El}{0.495}\right)} \tag{8}$$

The net fossil CO_2 emissions include direct and indirect fossil CO_2 emissions (Scope 1 and Scope 2) linked to the e-methanol production process, to which the captured CO_2 is subtracted (since it is assumed to be geologically stored with a BECCS approach). The net fossil CO_2 emissions, $NET_{fossil,CO2}$, are evaluated as in equation (9), where *El* is the specific electricity import of the plant (per tonnes of methanol), *EF* is the Emission Factor of the Italian electricity mix, equal to 0.268 t/MWh [64], and $CO_{2\ capture}$ is the amount of CO_2 captured by the CO_2 separation unit (per tonnes of methanol).

$$NET_{fossil,CO2}\left[\frac{t_{CO2}}{t_{MeOH}}\right] = El\left[\frac{MWh}{t_{MeOH}}\right] \cdot EF\left[\frac{t_{CO2}}{MWh}\right] - CO_{2\ capture}\left[\frac{t_{CO2}}{t_{MeOH}}\right] \tag{9}$$

The net fossil CO_2 emissions are negative in the four scenarios with CO_2 capture, i.e., the plants reduce the net CO_2 content in the atmosphere provided that, (i) captured CO_2 is sent to permanent storage (CCS) and, (ii) the biogenic carbon provided by the biomass feedstock is regenerated into new biomass stock at least with the same consumption rate of the residual biomass (typical assumption when residual biomass is used): as a result, the amount of permanently removed CO_2 is greater than the fossil CO_2 emissions associated to the electricity consumption of the plant. Net CO_2 emissions are equal to −1.81 t_{CO2}/t_{MeOH} in LOW-P (RC) scenario, −1.84 t_{CO2}/t_{MeOH} in LOW-P scenario, −1.64 t_{CO2}/t_{MeOH} in HIGH-P(RC) scenario and −1.66 t_{CO2}/t_{MeOH} in HIGH-P scenario. When low-pressure gasification is considered, the negative contribution given by the $CO_{2\ capture}$ term (t_{CO2}/t_{MeOH}) is greater than in high-pressure gasification scenarios, given the greater amount of CO_2 removed from the syngas and the lower quantity of methanol produced. This occurs even though the low-pressure gasification scenarios have greater electricity consumption (and related CO_2 emissions). In scenario *H_2-ADD* the net fossil CO_2 emissions are positive (1.64 t_{CO2}/t_{MeOH}), as CO_2 capture is absent in this process and the consumed electricity is assumed to be produced at the average CO_2 intensity of the grid. In this scenario the emissions are totally associated to the high electricity consumption of the electrolyzer and assuming a decarbonization of the electricity grid the CO_2 emissions can be drastically reduced (they would be zero for 100%-renewable electricity). Although it represents a useful estimation of the direct and indirect fossil CO_2 emissions, such calculation is not meant to replace a detailed LCA analysis, which would be still required to rigorously assess the overall GHGeq footprint of the different scenarios on a lifecycle basis.

The syngas flow rate at inlet of the methanol synthesis reactor and methanol productivity are maximum in the *H_2-ADD* scenario, where no CO_2 is removed and H_2 is added. In the scenarios with CO_2 removal the methanol production is nearly similar across the four cases; it is greater in *HIGH-P(RC)* given the lower CO_2 percentage in the syngas that favors the methanol yield [65], despite the syngas flow rate increases in the HIGH-P scenario where less CO_2 is removed.

The *CGE* is greater in *H_2-ADD* scenario since WGS is not required. *CGE* is greater for high-pressure than low-pressure gasification since, although the *CGE* of the gasifier island only would be worse, the high-temperature filtration entails a reduction of the O_2 consumption in the reforming step (−18 %) hence favoring the advanced scenarios. In the Reference Case scenarios (*LOW-P(RC)* and *HIGH-P(RC)*) the *CGE* is

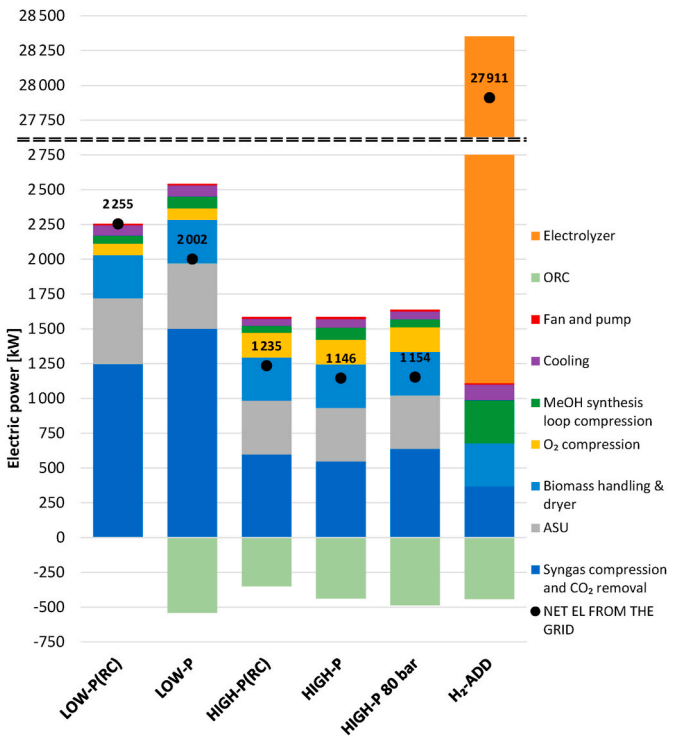

Fig. 6. Breakdown of the electricity consumption in the five alternative scenarios investigated. Negative contributions correspond to electricity produced within the plant. Notice the different (larger) scale in the H_2-ADD case.

greater than the corresponding advanced technological options (*LOW-P* and *HIGH-P*) given the greater WGS bypass set by the different downstream CO_2 removal technology chosen.

Concerning the four scenarios with CO_2 removal, the primary energy efficiency mainly depends on the gasification pressure, with values close to 50 % in high-pressure scenarios, due to the lower electricity consumption for syngas compression, dropping to 43–44 % in the low-pressure gasification case. The electricity consumption in scenario *HIGH-P(RC)* and *HIGH-P* is reduced by around 30–38 % compared to *LOW-P(RC)* and *LOW-P*. As shown in Fig. 6, where the energy consumption/production breakdown is reported, the contributions of the syngas compression and CO_2 removal sections to the electricity consumption of the plant are lower in the high-pressure scenarios than in low-pressure ones. The high-pressure scenarios have a larger O_2 compression consumption due to the higher gasification pressure. In the scenarios at low-pressure, where syngas compression has a significant impact on the electricity consumption, the compression of syngas after CO_2 removal (*LOW-P(RC)* case*)* reduces the total electricity consumption of the plant compared to *LOW-P* scenario. However, CO_2 removal with MEA has high thermal demand and no waste heat is available to be recovered by an ORC in this case and, as a result, the net electricity consumption of *LOW-P* is larger and the energy efficiency is lower than in the *LOW-P* scenario.

It is worth highlighting that *H_2-ADD* reports the lowest primary energy efficiency values among the considered scenarios: 33 %; as described in Fig. 6, this is mainly a result of the considerable increase in the electricity consumption, which raises from 1.1 to 2.2 MW in the CO_2 removal scenarios to 28 MW in *H_2-ADD*, due to the significant consumption, i.e. 27 MW of the H_2 electrolyzer.

The Carbon Efficiency indicator (also called carbon yield), reported in Table 8, reflects the amount of carbon kept in the output product, i.e. methanol, divided by the amount of carbon originally present in the input biomass. While the difference in the first four scenarios is mostly related to the gasification pressure (37.6 % at *LOW-P* vs nearly 40 % at *HIGH-P*), the considerably higher value for the *H_2-ADD* case, 93.8 %, highlights the role of H_2 addition, which leads to a significantly better exploitation of the carbon in the biomass (i.e., CO_2 removal is no longer needed since all the carbon in the syngas, except the one in the purge and off-gas streams, is converted into methanol) with a considerably greater methanol production.

The thermal integration of the whole biomass-to-methanol process is represented in the Temperature - Heat duty diagram (T-Q) of Fig. 7, referring to the best-case scenario *HIGH-P*.

Diagram (a) reports the T-Q diagram for the gasification section: from the hot syngas leaving the reformer to the CO_2 removal unit.

- the hot syngas leaving the reformer (before the desulfurization) is cooled in counter-current from 1000 °C to 200 °C by the following sequence of streams:
  - high-temperature steam is superheated (SH) from 250 °C to 400 °C before entering the gasifier;
  - high-temperature steam evaporates at 250 °C (EVA2), where the evaporation temperature is set by the operation temperature of the methanol synthesis reactor (see diagram (b));
  - diathermal oil for waste heat recovery (as the hot source for the ORC cycle);
  - liquid water to be pre-heated (ECO2);
  - fresh syngas to be pre-heated to 210 °C before entering the methanol synthesis loop;
  - low-temperature saturated steam generated at 120 °C (for distillation columns reboilers and biomass dryer);
- the hot syngas leaving the desulfurization system (before the WGS reactor) is further cooled from 350 °C to 200 °C by producing low-temperature saturated steam at 120 °C;
- the hot syngas leaving the WGS reactor at 350 °C heats up a diathermal oil stream for the ORC;
- the hot syngas leaving the water saturator is cooled from 150 °C to 130 °C by the following streams:
  - low-temperature saturated steam generated at 120 °C such that the total low-T steam produced covers both the duty of the biomass dryer (935 kW_{th}) and of the distillation columns reboilers (around 1300 MJ_{th}/t_{MeOH}, a value consistent with the literature [26,66,67]);
  - liquid water to be pre-heated (ECO1);
- the hot syngas leaving the compressor further pre-heats to 120 °C the syngas leaving the CO_2 separation unit.

Diagram (b) refers to the methanol synthesis island where the following heat integration is carried out.

- high-temperature steam is evaporated from saturated liquid to saturated vapor at 250 °C (EVA1) by keeping the methanol synthesis reactor under isothermal conditions;
- the gaseous product leaving the synthesis reactor are sequentially cooled by:
  - the recycle of methanol synthesis;
  - raw methanol before entering the purification section.

Diagram (c) refers to the vent and purge gas boiler which provides heat to the following streams.

- diathermal oil for the ORC cycle;
- combustion air to be pre-heated until 250 °C.

In scenarios with CO_2 capture based on absorption with solvent (*LOW-P(RC)* and *HIGH-P(RC)*), heat is needed to regenerate the solvent. Thermal power for the MDEA or MEA reboiler is provided by low-temperature saturated steam at 120 °C; therefore, in these cases the waste heat available for the ORC is very limited or not enough to justify the installation of an ORC, such as in the MEA *LOW-P(RC)* scenario.

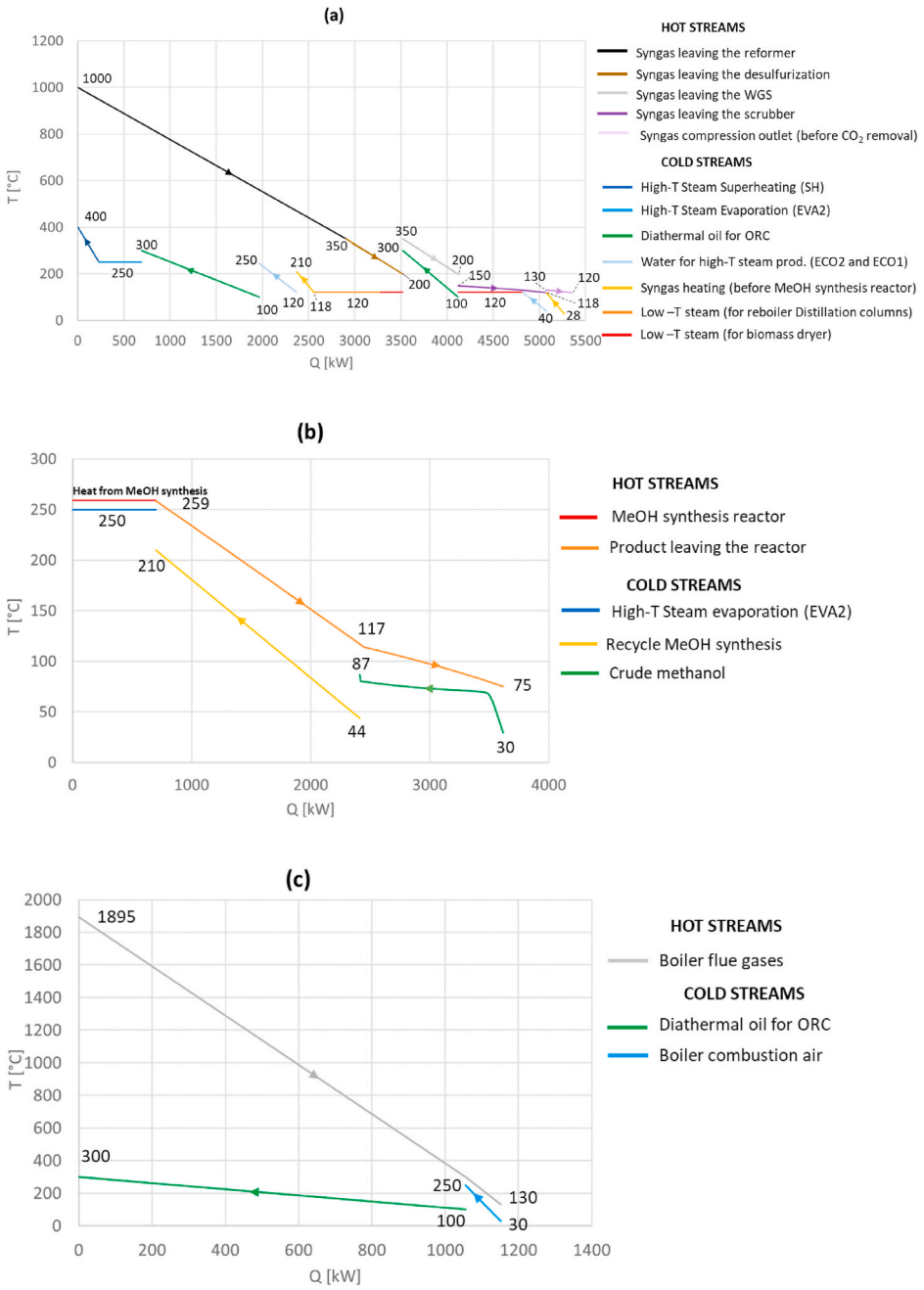

Fig. 7. Temperature-Heat duty (T–Q) diagrams of the HIGH-P process: hot syngas (a), methanol synthesis loop (b) and off-gas boiler (c) sections.

5.2. Economic analysis results

The results of the economic analysis are summarized in Table 9 in terms of Levelized Cost of Methanol (*LCOM*), capital expenditure of the plant (*CAPEX*) and the operational expenditure (*OPEX*), for the five alternative scenarios.

The best scenario from an economic point of view is the *HIGH-P* scenario with high-pressure gasification and low-temperature CO_2 removal. In the *HIGH-P* scenario the LCOM is equal to 700 €/t_{MeOH} and both the *CAPEX* and *OPEX* are lower than in other options. The *HIGH-P (RC)* scenario is second in the ranking because, although it has comparable *CAPEX* and *OPEX* to the low-pressure scenarios, its slightly increased production of methanol reduces the *LCOM*.

The *CAPEX* reduction in *HIGH-P* scenarios is mainly given by the low cost of the syngas treatment section: the cost of the syngas compression section is lower than in the *LOW-P* scenarios thanks to the high-pressure gasification, and the CO_2 removal units have lower cost than the *HIGH-P (RC)* scenario given the simplicity of the cryogenic heat exchanger compared to the solvent absorption system. The main contribution to the *CAPEX* is given by the gasification section with a cost ranging from 27 to 31 M€, with the largest cost characterizing the high-pressure gasification cases.

The *OPEX* is lower in the *HIGH-P* scenario due to the lower electricity consumption for syngas compression and the greater electricity production by ORC compared to the Reference Case (RC) scenarios. The electricity consumption contributes to 13–22 % of the *OPEX*, the biomass cost for 30–35 % and the fixed cost for (34–38 %). Differently, the scenario with H_2 addition (*H_2-ADD*) is significantly influenced by the electricity cost, which accounts for 77 % of *OPEX*.

Fig. 8, reporting the different contributions to the *LCOM*, highlights the great impact of the H_2 production cost (equal to 5.3 €/kg_{H2} in this study) on the *LCOM* for the *H_2-ADD* scenario, while all other costs (e.g.,

Table 9
Results of the economic analysis with CAPEX and OPEX breakdown for the alternative five biomass-to-methanol scenarios.

SCENARIOS		LOW-P (RC)	LOW-P	HIGH-P (RC)	HIGH-P	H_2-ADD
MeOH produced	t/y	14481	14449	15435	15337	36083
LCOM	€/t	831	792	730	700	821
CAPEX	M€	57.0	53.9	56.6	53.0	64.5
ASU	*M€ (%)*	*14.5 (25 %)*	*15.7 (29 %)*	*13.7 (24 %)*	*14.9 (28 %)*	-
Gasification section	*M€ (%)*	*27.3 (48 %)*	*27.9 (52 %)*	*30.2 (53 %)*	*30.6 (58 %)*	*30.0 (46 %)*
Syngas treatment	*M€ (%)*	*12.6 (22 %)*	*5.2 (10 %)*	*8.7 (15 %)*	*2.7 (5 %)*	*2.1 (3 %)*
Electrolyzer		-	-	-	-	*23.7 (37 %)*
ORC	*M€ (%)*	-	*2.1 (4 %)*	*1.5 (3 %)*	*1.8 (3 %)*	*1.8 (3 %)*
MeOH synthesis section	*M€ (%)*	*2.6 (5 %)*	*3.0 (6 %)*	*2.5 (4 %)*	*3.1 (6 %)*	*6.9 (11 %)*
OPEX	M€/y	6.7	6.4	6.0	5.8	23.6
Biomass	*M€/y (%)*	*2.0 (30 %)*	*2.0 (31 %)*	*2.0 (34 %)*	*2.0 (35 %)*	*2.0 (9 %)*
CO_2 transport and storage	*M€/y (%)*	*0.31 (5 %)*	*0.31 (5 %)*	*0.28 (5 %)*	*0.28 (5 %)*	-
Electricity	*M€/y (%)*	*1.5 (22 %)*	*1.3 (20 %)*	*0.8 (14 %)*	*0.8 (13 %)*	*18.3 (77 %)*
Labor	*M€/y (%)*	*0.5 (8 %)*	*0.5 (8 %)*	*0.5 (9 %)*	*0.5 (9 %)*	*0.5 (2 %)*
Fixed OPEX	*M€/y (%)*	*2.3 (34 %)*	*2.2 (34 %)*	*2.3 (38 %)*	*2.1 (37 %)*	*2.6 (11 %)*
Other	*M€/y (%)*	*0.08 (1 %)*	*0.08 (1 %)*	*0.07 (1 %)*	*0.07 (1 %)*	*0.19 (1 %)*

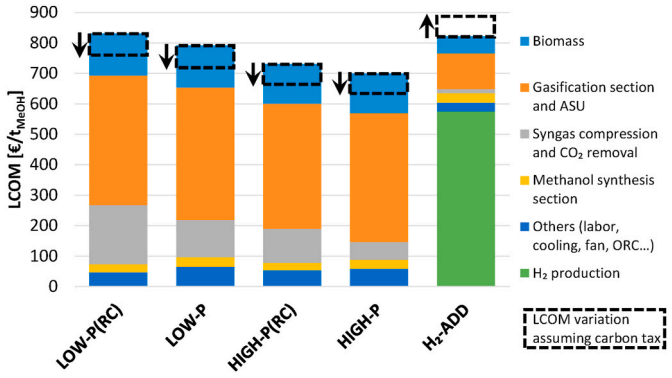

Fig. 8. The different contributions to the LCOM in the alternative five scenarios. Carbon tax/credit is assumed equal to 40 €/t_{CO2}.

ASU, gasification, synthesis) are reduced on a specific basis, since they are distributed over a greater amount of methanol produced compared to scenarios with CO_2 capture, i.e., 36 kt/y against 14–15 kt/y. For *H_2-ADD*, the main contribution is given by the *OPEX* for electricity consumption, while from the *CAPEX* standpoint the main item remains the gasification island (46 % of *CAPEX*), followed by the electrolyzer cost (37 % of *CAPEX*). If the potential sale of the extra O_2 produced by the electrolyzer and not yet auto-consumed in the plant (assuming a 100 €/t_{O2} selling price) is considered, then the *LCOM* of scenario *H_2-ADD* is reduced from 821 €/t_{MeOH} to 770 €/t_{MeOH}.

In the scenarios with CO_2 removal, Fig. 8 shows the reduction of the contribution given by the syngas treatment section from *LOW-P(RC)* scenario to *HIGH-P* scenario. According to the economic analysis, the process based on high pressure gasification and low temperature CO_2 removal (*HIGH-P*) stands out as the lowest cost one, with a potential to reduce the *LCOM* cost to 700 €/t_{MeOH} from 831 €/t_{MeOH} of the benchmark case.

Afterwards, the variation of the *LCOM* given by the application of a carbon tax/credit scheme is evaluated, assuming a carbon tax equal to 40 €/t_{CO2} (average price [68] representative of the pre-pandemic scenario and currently much lower than the 2022 yearly average, but coherent with the baseline year assumed for costing, 2020) charged to the net fossil CO_2 emissions for each scenario. In scenarios with CO_2 removal and negative net fossil CO_2 emissions, the *LCOM* is reduced by around 9 % without changing the ranking among the options (759 €/t_{MeOH} in *LOW-P(RC)* scenario, 719 €/t_{MeOH} in *LOW-P* scenario, 664 €/t_{MeOH} in *HIGH-P(RC)* scenario and 633 €/t_{MeOH} in *HIGH-P* scenario).

On the other hand, *H_2-ADD* features positive net fossil CO_2 emissions at current CO_2 intensities of the Italian grid, resulting in a *LCOM* increase to 886 €/t_{MeOH} (+8 %).

In any case, for all the analyzed bio-methanol production processes, *LCOM* does not seem competitive with the current market price of fossil methanol equal to 329 €/t_{MeOH} (average 2019 selling price [69]), even if this is increased to 415 €/t_{MeOH} by the carbon tax application. As a reference, average CO_2 emissions for fossil methanol production from natural gas are 2.14 t_{CO2}/t_{MeOH} (1.38 t_{CO2}/t_{MeOH} are related to MeOH carbon content, plus 0.06 t_{CO2}/t_{MeOH} by indirect emission for electricity production, plus 0.7 t_{CO2}/t_{MeOH} by direct emissions from the fossil fuel consumption [67]). However, the outcome of the comparison could change if we consider the year 2022 situation, in which both the carbon tax and the cost of fossil methanol has increased, respectively, up to 90 €/t_{CO2} and 500 €/t_{MeOH}, potentially favoring the competitiveness of bio-methanol with negative emissions against fossil methanol.

5.2.1. *Sensitivity*

A sensitivity analysis is conducted to evaluate the impact of the main economic assumptions on the *LCOM*.

The cost of biomass can vary widely, depending on the type of biomass and its origin [70]. The graph on Fig. 9, left-hand side, reports the variation of *LCOM* with the cost of the biomass, which significantly affects the scenarios with CO_2 removal (*LOW-P(RC)*, *LOW-P*, *HIGH-P (RC)*, *HIGH-P*) and to a lesser extent the scenario with H_2 addition (*H_2-ADD*). In case the cost of biomass more than doubles (to 150 €/t (left)) with respect to the base case (68 €/t), the LCOM of the scenarios with CO_2 removal increases between 8 % (*H_2-ADD* scenario) and 20 % (best case scenario *HIGH-P*).

In the *H_2-ADD* scenarios, the *OPEX* is highly affected by the cost of electricity consumption, as shown in the graph on Fig. 9 right-hand side,. If the electricity cost (83 €/MWh in the base case) increases to 200 €/MWh, the *LCOM* of *H_2-ADD* scenario increases to 1534 €/t_{MeOH} (+87 % with respect to the base case), expanding the gap with scenarios with CO_2 removal. The scenarios with CO_2 removal increase by nearly 16 % with low-pressure gasification and by about 10 % in scenarios with low-pressure gasification. On the other hand, the *H2-ADD* scenarios is the most economically promising if electricity is available at a cost lower than 60 €/MWh. The cost of H_2 should be reduced from 5.3 €/kg_{H2} (base case) to 4.2 €/kg_{H2} to get the *LCOM* of *H_2-ADD* equal to the one of the *HIGH-P* scenario.

Given the limited commercial maturity of the *HIGH-P* scenarios, a sensitivity analysis is conducted varying the cost of the high-pressure gasification and the low temperature CO_2 removal section one. In

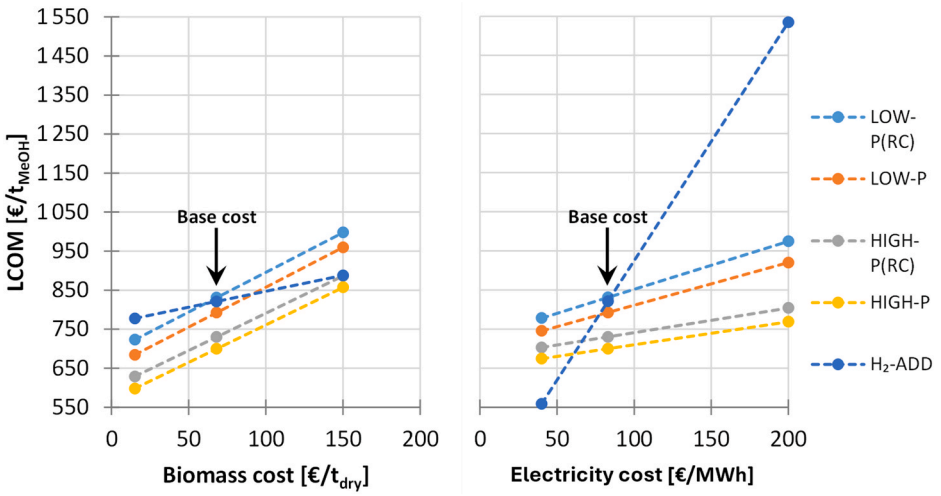

Fig. 9. Sensitivity variation of the LCOM with the biomass cost (left) and electricity purchase price on the market (right).

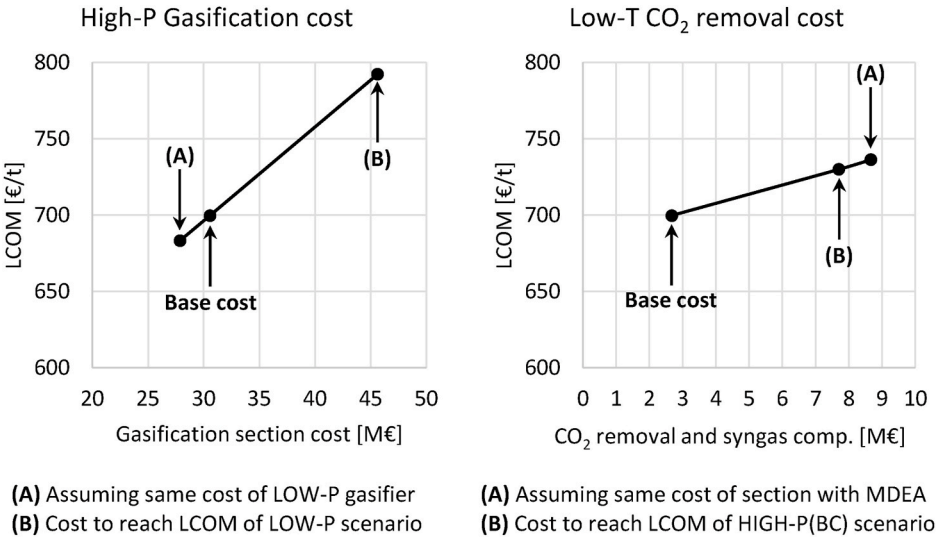

Fig. 10. Sensitivity variation of the LCOM in HIGH-P scenario as a function of the cost of high-pressure gasification (left) and low-temperature CO_2 removal section (right).

Fig. 10 the *LCOM* of *HIGH-P* scenario is reported varying the cost of the gasification section (left-hand side) and the syngas treatment section (right-hand side).

About the cost of the high-pressure gasification, if the same cost of the low-pressure gasification is considered (point A), the *LCOM* is reduced to 680 €/t. The *LCOM* of the *HIGH-P* scenario becomes comparable to the *LCOM* of the *LOW-P* scenario (point B) if the CAPEX of *HIGH-P* gasification raises from 30 M€ (base case) to 45 M€, i.e., increasing the cost by 50 % (+64 % with respect to the low-pressure gasification cost).

As shown in the graph on the right in Fig. 10, the *LCOM* of the *HIGH-P* scenario becomes comparable to the *HIGH-P(RC)* scenario (point B) if the cost of the syngas compression and low temperature CO_2 removal section increases to 7.7 M€ (+188 % with respect to the estimated cost); therefore, to replace traditional solvent-based CO_2 absorption with low-temperature CO_2 separation seems economically advantageous even in case the cost of the latter is doubled compared to the assumed cost.

6. Conclusions

This paper presents a techno-economic assessment of five different plant configurations aimed at producing bio-methanol starting from the gasification of residual lignocellulosic biomass. A first principle Fluidized Bed Gasifier model is presented and calibrated based on literature data. The case studies are all based on the same biomass input flow rate, i.e. 19 MW_{th}, and differ from the point of view of (i) the gasification pressure, (ii) the CO_2 capture technology, since amine scrubbing is assumed as a benchmark, while low-temperature separation via phase-change is used as novel technology, (iii) the possible addition of H_2 from electrolysis to maximize the methanol output (case *H_2-ADD*). Process configurations are defined to maximize the methanol production while matching the constraints on the operational conditions of the gasification and methanol synthesis island, as well as on the stoichiometric ratio (or module) and maximum amount of inerts in the syngas. Thermal integration is performed in order to satisfy the thermal demand of the process in terms of heat for methanol purification, steam generation for gasification, with the minimum number of heat exchanger units. Residual waste heat from the process, if any, is exploited in an ORC plant to partly offset the electricity consumption from the grid.

Four cases entail Carbon Capture and Storage, while a fifth one aims at converting all the carbon in the syngas into methanol through the addition of H_2 from electrolysis. All the cases with CO_2 capture feature

negative net fossil CO_2 emissions and can therefore be considered plants producing biomethanol with negative emissions (or carbon dioxide removal, CDR), since the capture of biogenic CO_2 (assumed here to be then transported and sent to geological storage) more than offsets the indirect (scope 2) CO_2 emissions coming from the fossil share of the electricity mix: −1.81 t_{CO2}/t_{MeOH} in *LOW-P(RC)* scenario, −1.84 t_{CO2}/t_{MeOH} in *LOW-P* scenario, −1.64 t_{CO2}/t_{MeOH} in *HIGH-P(RC)* scenario, −1.66 t_{CO2}/t_{MeOH} in *HIGH-P* scenario. The only case with positive fossil CO_2 emissions is *H_2-ADD*, which indirectly emits 1.64 t_{CO2}/t_{MeOH}, assuming that H_2 is not of completely green origin but it is produced with the average electricity mix of Italy.

From the point of view of the thermodynamic performance, the best case scenarios in terms of primary energy efficiency are the ones with pressurized gasification ($\eta_{primary,en}$ equal to 50 %), since they benefit from a great reduction in the electric power consumed from syngas compression. The CCS-based cases produce very similar amounts of methanol (between 14449 t/y and 15435 t/y), while their methanol production cost is minimum in the *HIGH-P* case, where it is equal to 700 €/t_{MeOH} and increases up to 730 €/t_{MeOH} when a conventional MDEA capture technology is used in place of the low-temperature phase separation; on the other hand, when a lower gasification pressure is conservatively chosen, OPEX increase by around 10 % and, as a result *LCOM* increases up to 792 €/t_{MeOH} or 831 €/t_{MeOH} (depending on the CCS technology), due to the greater compression power required to bring the syngas from gasification to the methanol synthesis pressure (i.e., 60 bar). Despite the presence of a small ORC power plant, with sizes varying from 351 kW to 556 kW, all the scenarios are net consumers of electricity, with net electricity consumption ranging from 1150 kW to 2255 kW, increasing up to 28 MW_{el} in the electrolysis-based plant.

CAPEX of the CCS-based plants is not significantly affected by an increase of pressure, since the greater cost of the gasification island (increased by 10 % when the pressure is raised from 2.5 bar to 28 bar) is estimated to be compensated by the reduction of the syngas compressors size and cost; by contrast the CCS technology affects the *CAPEX* and *OPEX*, since the low-temperature CO_2 separation technology is expected to reduce the capital cost by around 3 M€ and to import less electricity, as a result of the synergies with the gasification and methanol production sections.

A sensitivity analysis highlights that: for every 50 €/t increase in the biomass fuel costs, the *LCOM* raises by around 100 €/t_{MeOH} (with an halved impact just for the *H_2-ADD* case that features a nearly doubled productivity in terms of methanol-to-biomass ratio); *LCOM* is very sensitive to the electricity price, in particular in the *H_2-ADD* scenario, in which the increase of electricity price to 200 €/MWh leads to a *LCOM* of 1536 €/t_{MeOH} and a reduction to 60 €/MWh reduces the *LCOM* to 681 €/t_{MeOH} (making this scenario the most economically promising); the uncertainty on the cost of the high pressure gasifier may affect the *LCOM* ranking, *LCOM* of the *HIGH-P* case becomes equal to the *LCOM* of the low-pressure scenario when the high pressure gasifier cost is increased from 31 M€ to 46 M€ (+48 %); on the other hand, the cost of the CO_2 removal section has lower impact on the *LCOM* and the scenario with the low-temperature CO_2 separation reaches the *LCOM* of the scenario with conventional CO_2 removal if the cost of the CO_2 removal section increases considerably from 2.7 M€ a 7.7 M€ (+188 %).

Among the five plant configurations investigated, the reference case based on low gasification pressure and amine capture (*LOW-P(RC)*) is the most mature and, likely, appropriate for building a demonstration plant, while, in perspective, the case with higher gasification pressure and CO_2 capture via low-temperature CO_2 separation (*HIGH-P*) has the best efficiency and greatest techno-economic potential, although affected by a lower technological maturity. The hydrogen-based option (*H_2-ADD*) is worth considering just in case low-cost decarbonized green H_2 (namely, 100 % RES electricity and at costs lower than 65 €/MWh) is available, a target which seems challenging to reach in the short-term, in the investigated context.

CRediT authorship contribution statement

Giorgia Lombardelli: Writing – original draft, Methodology, Formal analysis, Software, Data curation, Visualization. **Roberto Scaccabarozzi:** Writing – review & editing, Data curation, Conceptualization, Validation. **Antonio Conversano:** Writing – review & editing, Data curation, Conceptualization, Validation. **Manuele Gatti:** Funding acquisition, Conceptualization, Methodology, Writing – review & editing, Validation, Supervision.

Data availability

Data will be made available on request.

Acknowledgments

The Emilia-Romagna Region (Delibera di Giunta Regionale 769/2018) and the EU are acknowledged for funding the PhD scholarship (soggetto attuatore: Politecnico di Milano) of Giorgia Lombardelli entitled “Sviluppo di tecnologie criogeniche per la produzione di biometano liquido a partire da biogas”, Rif. P.A. n° 2018–10680/RER, CUP D36C19000080005 (POR FSE 2014/2020). This study was also partly conducted in collaboration with the Agritech National Research Center, in the framework of which Manuele Gatti and POLIMI received funding from the European Union Next-GenerationEU (PIANO NAZIONALE DI RIPRESA E RESILIENZA (PNRR) – MISSIONE 4 COMPONENTE 2, INVESTIMENTO 1.4 – D.D. 1032 June 17, 2022, CN00000022). This manuscript reflects only the authors’ views and opinions, neither the European Union nor the European Commission can be considered responsible for them.

Appendix A. Supplementary data

Supplementary data to this article can be found online at https://doi.org/10.1016/j.biombioe.2024.107315.

References

[1] International Energy Agency, World Energy Outlook 2022, 2022.
[2] International Energy Agency, Net Zero by 2050: A Roadmap for the Global Energy Sector, 2021.
[3] H. Zhang, L. Wang, J. Van, F. Maréchal, U. Desideri, Techno-economic evaluation of biomass-to-fuels with solid-oxide electrolyzer 270 (April) (2020).
[4] International Renewable Energy Agency and Methanol Institute, INNOVATION OUTLOOK Renewable Methanol, 2021.
[5] M. Pérez-Fortes, E. Tzimas, “Techno-economic and environmental evaluation of CO2 utilisation for fuel production, Synthesis of methanol and formic acid.,” (2016), https://doi.org/10.2790/89238.
[6] A. Giuliano, et al., Towards methanol economy: a techno-environmental assessment for a bio-methanol OFMSW/biomass/carbon capture-based integrated plant, International Journal of Heat and Technology 37 (3) (2019) 665–674, https://doi.org/10.18280/ijht.370301.
[7] P. Galindo Cifre, O. Badr, Renewable hydrogen utilisation for the production of methanol, Energy Convers. Manag. 48 (2) (2007) 519–527, https://doi.org/10.1016/j.enconman.2006.06.011.
[8] E. Peduzzi, L. Tock, G. Boissonnet, F. Marechal, Thermo-economic evaluation and optimization of the thermo-chemical conversion of biomass into methanol, Proceedings of the 25th International Conference on Efficiency, Cost, Optimization and Simulation of Energy Conversion Systems and Processes, ECOS 2012 3 (2012) 333–345.
[9] J. Hrbek, Status Report on Thermal Biomass Gasification in Countries Participating in IEA Bioenergy Task, 33, 2016.
[10] F. Duan, B. Jin, Y. Huang, B. Li, Y. Wu, M. Zhang, Results of bituminous coal gasification upon exposure to a pressurized pilot-plant circulating fluidized-bed (CFB) reactor, Energy Fuel. 24 (5) (2010) 3150–3158, https://doi.org/10.1021/ef901596n.
[11] E. Kurkela, J. Laatikainen-Luntama, P. Ståhlberg, A. Moilanen, Pressurised fluidised-bed gasification experiments with biomass, peat and coal at VTT in 1991-1994: Part 3. Gasification of Danish Wheat Straw and Coal, 1996, p. 291.
[12] Wiebren de Jong, J. Andries, K.R.G. Hem, COAL/BIOMASS CO-gasification in a pressurised fluidised bed reactor, Renew. Energy 16 (1999) 1110–1113.
[13] C.N. Hamelinck, A.P.C. Faaij, Future prospects for production of methanol and hydrogen from biomass, J. Power Sources 111 (1) (2002) 1–22, https://doi.org/10.1016/S0378-7753(02)00220-3.

[14] L.R. Clausen, N. Houbak, B. Elmegaard, Technoeconomic analysis of a methanol plant based on gasification of biomass and electrolysis of water, Energy 35 (5) (2010) 2338–2347, https://doi.org/10.1016/j.energy.2010.02.034.
[15] I. Hannula, Co-production of synthetic fuels and district heat from biomass residues, carbon dioxide and electricity: performance and cost analysis, Biomass Bioenergy 74 (2015) 26–46, https://doi.org/10.1016/j.biombioe.2015.01.006.
[16] I. Hannula, E. Kurkela, Liquid Transportation Fuels via Large-Scale Fluidised-Bed Gasification of Lignocellulosic Biomass, January. 2013. VTT Technology 91.
[17] A. Giuliano, C. Freda, E. Catizzone, Techno-economic assessment of bio-syngas production for methanol synthesis: a focus on the water–gas shift and carbon capture sections, Bioengineering 7 (3) (2020) 1–18, https://doi.org/10.3390/bioengineering7030070.
[18] I. Hannula, E. Kurkela, A parametric modelling study for pressurised steam/O 2-blown fluidised-bed gasification of wood with catalytic reforming, Biomass Bioenergy 38 (2012) 58–67, https://doi.org/10.1016/j.biombioe.2011.02.045.
[19] V. Dieterich, A. Buttler, A. Hanel, H. Spliethoff, S. Fendt, Power-to-liquid via synthesis of methanol, DME or Fischer–Tropsch-fuels: a review, Energy Environ. Sci. 13 (10) (2020) 3207–3252, https://doi.org/10.1039/d0ee01187h.
[20] D.A. Chisalita, C.C. Cormos, Techno-economic assessment of hydrogen production processes based on various natural gas chemical looping systems with carbon capture, Energy 181 (2019) 331–344, https://doi.org/10.1016/j.energy.2019.05.179.
[21] T.G. Kreutz, E.D. Larson, G. Liu, R.H. Williams, Fischer-tropsch fuels from coal and biomass, in: 25th Annual International Pittsburgh Coal Conference, PCC - Proceedings, August 2008.
[22] D. Shekhawat, J.J. Spivey, D.A. Berry, Fuel Cells: Technologies for Fuel Processing 2011, first ed., Elsevier, 2011.
[23] M. Gatti, Multi-objective Optimization of Novel CO2 Capture Processes for Gasification Based Plants, Politecnico di Milano, 2014.
[24] D. Berstad, J. Straus, T. Gundersen, CO2 capture and enhanced hydrogen production enabled by low-temperature separation of PSA tail gas: a detailed exergy analysis, Energies 17 (5) (Feb. 2024) 1072, https://doi.org/10.3390/en17051072.
[25] X. Cui, S.K. Kær, A comparative study on three reactor types for methanol synthesis from syngas and CO2, Chem. Eng. J. 393 (October 2019) (2020), https://doi.org/10.1016/j.cej.2020.124632.
[26] J. Nyári, M. Magdeldin, M. Larmi, M. Järvinen, A. Santasalo-Aarnio, Techno-economic barriers of an industrial-scale methanol CCU-plant, J. CO2 Util. 39 (May) (2020), https://doi.org/10.1016/j.jcou.2020.101166.
[27] V. Pethurajan, S. Sivan, G.C. Joy, Issues, comparisons, turbine selections and applications – an overview in organic Rankine cycle, Energy Convers. Manag. 166 (Jun. 2018) 474–488, https://doi.org/10.1016/j.enconman.2018.04.058.
[28] ARPAE, Rapporto Energia Dell ' Emilia -Romagna, 2020.
[29] Regione Emilia Romagna, Cartografia interattiva del Sistema Informativo Forestale regionale [Online]. Available: https://servizimoka.regione.emilia-romagna.it/mokaApp/apps/FORESTEHTM5/index.html. (Accessed 19 January 2024).
[30] European Commision, Phyllis database [Online]. Available: https://phyllis.nl/Browse/Standard/ECN-Phyllis. (Accessed 19 January 2024).
[31] AspenTech, Aspen plus [Online]. Available: https://www.aspentech.com/en. (Accessed 19 January 2024).
[32] Barr-Rosin, "Superheated steam drying, Energy integration.".
[33] L. Fagernäs, J. Brammer, C. Wilén, M. Lauer, F. Verhoeff, Drying of biomass for second generation synfuel production, Biomass Bioenergy 34 (9) (Sep. 2010) 1267–1277, https://doi.org/10.1016/j.biombioe.2010.04.005.
[34] A. Poluzzi, et al., Flexible power and biomass-to-methanol plants with different gasification technologies, Front. Energy Res. 9 (January) (2022) 1–23, https://doi.org/10.3389/fenrg.2021.795673.
[35] S.M. Gibson, Oxygen Plants for Gasification, New Horizons Gasification, 2014, pp. 1–9.
[36] G. Beysel, T. Schueler, The proven cryogenic Air Separation Process adapted to the needs of CCS (IGCC & Oxyfuel). 10th European Gasification Conference, 2010.
[37] G. Butera, R.Ø. Gadsbøll, G. Ravenni, J. Ahrenfeldt, U.B. Henriksen, L.R. Clausen, Thermodynamic analysis of methanol synthesis combining straw gasification and electrolysis via the low temperature circulating fluid bed gasifier and a char bed gas cleaning unit, Energy 199 (2020), https://doi.org/10.1016/j.energy.2020.117405.
[38] S. Valin, S. Ravel, J. Guillaudeau, S. Thiery, Comprehensive study of the influence of total pressure on products yields in fluidized bed gasification of wood sawdust, Fuel Process. Technol. 91 (10) (2010) 1222–1228, https://doi.org/10.1016/j.fuproc.2010.04.001.
[39] O. Fandino, J.P.M. Trusler, D. Vega-Maza, Phase behavior of (CO 2 + H 2) and (CO 2 + N 2) at temperatures between (218 . 15 and 303 . 15) K at pressures up to 15 MPa, International Journal fo Greenhouse Gas Control 36 (2015) 78–92.
[40] J. Husebye, A.L. Brunsvold, S. Roussanaly, X. Zhang, Techno economic evaluation of amine based CO 2 capture : impact of CO 2 concentration and steam supply 23 (1876) (2012) 381–390, https://doi.org/10.1016/j.egypro.2012.06.053.
[41] M.C. Romano, P. Chiesa, G. Lozza, Pre-combustion CO2 capture from natural gas power plants, with ATR and MDEA processes, Int. J. Greenh. Gas Control 4 (5) (2010) 785–797, https://doi.org/10.1016/j.ijggc.2010.04.015.
[42] C. Antonini, J.F. Pérez-Calvo, M. van der Spek, M. Mazzotti, Optimal design of an MDEA CO2 capture plant for low-carbon hydrogen production — a rigorous process optimization approach, Sep. Purif. Technol. 279 (July) (2021), https://doi.org/10.1016/j.seppur.2021.119715.
[43] M. Asif, X. Gao, H. Lv, X. Xi, P. Dong, Catalytic hydrogenation of CO2 from 600 MW supercritical coal power plant to produce methanol: a techno-economic analysis, Int. J. Hydrogen Energy 43 (5) (2018) 2726–2741, https://doi.org/10.1016/j.ijhydene.2017.12.086.
[44] G.H. Graaf, P.J.J.M. Sijtsema, E.J. Stamhuis, G.E.H. Joosten, Chemical equilibria in methanol synthesis, Chem. Eng. Sci. 41 (11) (1986) 2883–2890, https://doi.org/10.1016/0009-2509(86)80019-7.
[45] A.A. Kiss, J.J. Pragt, H.J. Vos, G. Bargeman, M.T. de Groot, Novel efficient process for methanol synthesis by CO2 hydrogenation, Chem. Eng. J. 284 (2016) 260–269, https://doi.org/10.1016/j.cej.2015.08.101.
[46] G. Bozzano, F. Manenti, Efficient methanol synthesis: perspectives, technologies and optimization strategies, Prog. Energy Combust. Sci. 56 (2016) 71–105, https://doi.org/10.1016/j.pecs.2016.06.001.
[47] R. Rinaldi, G. Lombardelli, M. Gatti, C.G. Visconti, M.C. Romano, Techno-economic analysis of a biogas-to-methanol process: study of different process configurations and conditions, J. Clean. Prod. 393 (July 2022) 136259, https://doi.org/10.1016/j.jclepro.2023.136259, 2023.
[48] S. Campanari, P. Chiesa, G. Manzolini, S. Bedogni, Economic analysis of CO2 capture from natural gas combined cycles using Molten Carbonate Fuel Cells, Appl. Energy 130 (2014) 562–573, https://doi.org/10.1016/j.apenergy.2014.04.011.
[49] S.O. Gardarsdottir, et al., Comparison of technologies for CO 2 capture from cement production—Part 2: cost analysis, Energies 12 (3) (2019), https://doi.org/10.3390/en12030542.
[50] B. Stürmer, et al., Biosurf Project - D3.4, Determining the Feasibility Threshold for Tradable Biomethane Certificates, 2020.
[51] NETL, Cost and Performance Baseline for Fossil Energy and Natural Gas to Electricity Volume 1, Bituminous Coal Plants, 2013.
[52] D. Bellotti, M. Rivarolo, L. Magistri, A comparative techno-economic and sensitivity analysis of Power-to-X processes from different energy sources, Energy Convers. Manag. 260 (March) (2022), https://doi.org/10.1016/j.enconman.2022.115565.
[53] A. Mayyas, et al., Manufacturing Cost Analysis for Proton Exchange Membrane Water Electrolyzers, 2019.
[54] S. Lemmens, Cost engineering techniques & their applicability for cost estimation of organic rankine cycle systems, Energies 9 (7) (2016), https://doi.org/10.3390/en9070485.
[55] Thermoflow, "Thermoflex." Accessed: January. 19, 2024. [Online]. Available: https://www.thermoflow.com/.
[56] "toweringskills.".
[57] R. Turton, R.C. Bailie, W.B. Whiting, J.A. Shaeiwitz, D. Bhattacharyya, Analysis, Synthesis, and Design of Chemical Processes, fourth ed., 2012.
[58] S2Biom, "Tools for Biomass Chains.".
[59] ARERA." [Online]. Available: https://www.arera.it/it/index.htm.
[60] E. Smith, J. Morris, H. Kheshgi, G. Teletzke, H. Herzog, S. Paltsev, The cost of CO2 transport and storage in global integrated assessment modeling, Int. J. Greenh. Gas Control 109 (2021) 103367, https://doi.org/10.1016/j.ijggc.2021.103367.
[61] M.J. Bos, S.R.A. Kersten, D.W.F. Brilman, Wind power to methanol: renewable methanol production using electricity, electrolysis of water and CO2 air capture, Appl. Energy 264 (August 2019) (2020), https://doi.org/10.1016/j.apenergy.2020.114672.
[62] R. Rivera-Tinoco, et al., Investigation of power-to-methanol processes coupling electrolytic hydrogen production and catalytic CO2 reduction, Int. J. Hydrogen Energy 41 (8) (2016) 4546–4559, https://doi.org/10.1016/j.ijhydene.2016.01.059.
[63] J. Gorre, F. Ortloff, C. van Leeuwen, Production costs for synthetic methane in 2030 and 2050 of an optimized Power-to-Gas plant with intermediate hydrogen storage, Appl. Energy 253 (June) (2019), https://doi.org/10.1016/j.apenergy.2019.113594.
[64] ISPRA, *Fattori di Emissione Atmosferica di Gas a Effetto Serra nel Settore Elettrico Nazionale e nei Principali Paesi Europei*, 317/2020, 2020.
[65] B. Hernández, M. Martín, Optimal process operation for biogas reforming to methanol: effects of dry reforming and biogas composition, Ind. Eng. Chem. Res. 55 (23) (2016) 6677–6685, https://doi.org/10.1021/acs.iecr.6b01044.
[66] P. Battaglia, G. Buffo, D. Ferrero, M. Santarelli, A. Lanzini, Methanol synthesis through CO2capture and hydrogenation: thermal integration, energy performance and techno-economic assessment, J. CO2 Util. 44 (November 2020) (2021), https://doi.org/10.1016/j.jcou.2020.101407.
[67] M. Pérez-Fortes, J.C. Schöneberger, A. Boulamanti, E. Tzimas, Methanol synthesis using captured CO2 as raw material: techno-economic and environmental assessment, Appl. Energy 161 (2016) 718–732, https://doi.org/10.1016/j.apenergy.2015.07.067.
[68] Statistica, "Statistica, Average Closing Spot Prices of European Emission Allowances (EUA) from 2010 to 2021.".
[69] Methanex, "Methanex." Accessed: January. 19, 2024. [Online]. Available: https://www.methanex.com/.
[70] D.A. Agar, M. Svanberg, I. Lindh, D. Athanassiadis, Surplus forest biomass – the cost of utilisation through optimised logistics and fuel upgrading in northern Sweden, J. Clean. Prod. 275 (2020) 123151, https://doi.org/10.1016/j.jclepro.2020.123151.